HUMID

Report on uncertainty in the spread of drought in models.

Informe sobre la incertidumbre en la propagación de la sequía en los modelos.

Proyecto HUMID[1], Entregable 7.

Author(s)	Pere Quintana Seguí Anaïs Barella Ortiz Jaime Gaona
Date of initial version	24/09/2020
Date of final version	20/10/2020

Abstract

Drought diagnosis and forecasting are fundamental issues regarding hydrological management in Spain, where recurrent water scarcity periods are normal. Land-surface models (LSMs) could provide relevant information for water managers on how drought conditions evolve. Here, we explore the usefulness of LSMs driven by atmospheric analyses with different resolutions and accuracies in simulating drought and its propagation to precipitation, soil moisture and streamflow through the system. We also analyse how regional climate models (RCMs) represent meteorological, soil moisture, and hydrological drought as well as propagation from precipitation anomalies to soil moisture and streamflow anomalies. We perform simulations for the 1980-2014 period with SASER (5 km resolution) and LEAFHYDRO (2.5 km resolution), which are forced by the Spanish SAFRAN dataset (at 5km and 30km resolutions), and the global eartH2Observe datasets at 0.25 degrees (including the MSWEP precipitation dataset). We also evaluate three RCMs, CNRM-RCSM4, COSMO-CLM, and PROMES. All of the RCM simulations were obtained from the Med-CORDEX database and were forced with ERA-Interim. We produce standardized indices for precipitation (SPI), soil moisture (SSMI) and streamflow (SSI). The results show that the model structure uncertainty remains an important issue in current

[1] HUMID es un proyecto financiando por el Ministerio de Ciencia, Innovación y Universidades del Gobierno de España (código CGL2017-85687-R).

generation large-scale hydrological simulations based on LSMs and RCMs. This is true for both the SSMI and SSI. The differences between the simulated SSMI and SSI by different LSMs are large, and the propagation scales for drought regarding both soil moisture and streamflow are overly dependent on the model structure. RCMs improve meteorological drought representation but uncertainties are high also for SSMI and SSI. For LSMs, forcing datasets have an impact on the uncertainty of the results but, in general, this impact is not as large as the uncertainty due to model formulation.

Table of Contents

1. Introduction

Drought is an important climatic risk that can be exacerbated by anthropogenic warming (Samaniego et al., 2018; Marx et al., 2018) and water management (Wanders and Wada, 2015). It is the result of complex interactions among processes in the atmosphere, on the continental surface, and within human management (Van Loon, 2015; 2016). Drought has large social impacts on the society of the Iberian Peninsula due to the scarcity and high degree of the utilization of water resources (MMA, 2000). Due to the degree of exposure that Spanish society has to drought, it is necessary to improve our knowledge on drought. It is also necessary to develop tools that improve our monitoring and early warning capabilities to provide water managers with better information. Currently, there is still an insufficient amount of knowledge and adequate tools to manage drought effectively in many places.

The most common meteorological drought index is the standardized precipitation index (SPI) (McKee et al., 1993). For instance, the drought monitoring product of the AEMET (Agencia Estatal de Meteorolog´ıa) is based on the SPI. There are other indices that also include reference evapotranspiration (ETo), such as the Palmer Drought Severity Index (PDSI) (Palmer, 1965), Reconnaissance Drought Index (RDI) (Tsakiris et al., 2007), Standardized Precipitation Evapotranspiration Index (SPEI) (Vicente-Serrano et al., 2010; Begueria et al., 2014) and Standardized Palmer Drought Index (SPDI) (Ma et al., 2014). Begueria et al. (2014) and Vicente-Serrano et al. (2015) studied the sensitivity of drought indices to ETo and precipitation and found that each one has a different sensitivity to each variable, which must be taken into account for practical applications, specifically if they are related to climate change (Sheffield et al., 2012). Similar to the SPI, standardized indices of other variables, such as soil moisture or streamflow (Farahmand and AghaKouchak, 2015), can be generated. In addition, these can be used to study how drought propagates throughout the system by correlating indices at different time scales (Barker et al., 2015).

Standardized soil moisture, if it was widely observed, would be a good drought indicator, as it integrates the balance among actual evapotranspiration, effective precipitation and other relevant processes and, in addition, it is directly linked to vegetation and is the water source that plants use. However, observed data for this variable are rare (Seneviratne et al., 2010). AghaKouchak et al. (2015) considers that satellite data, which are not currently used for drought monitoring in most basins, offer interesting opportunities to improve early drought warning, and Lines et al. (2017) shows that satellite data can be used for the early warning of droughts in the Ebro basin. Concerning remotely sensed soil moisture, recent missions (Entekhabi et al., 2010; Kerr et al., 2012; Bindlish et al., 2015) and new high-resolution datasets (Escorihuela et al., 2012; Merlin et al., 2013; Molero et al., 2016) are producing even more possibilities.

As precipitation deficits propagate through the hydrological system (Wilhite, 2000; Van Loon et al., 2012b), drought types are interrelated. Soil moisture drought is slightly out of phase with meteorological drought in non-irrigated areas and depends on several factors, such as the soil type and capacity to retain water as well as actual evapotranspiration. This is also applicable to regions where irrigation is carried out under unusual circumstances, for

example, to avoid crop loss. In irrigated areas, soil moisture drought is directly related to the availability of irrigation water and therefore depends on hydrological drought. Hydrological drought is also affected by meteorological drought but generally at a larger temporal scale than soil moisture drought. Therefore, each system component is characterized by its own propagation dynamics and memory.

A better understanding of the different types of drought and their propagation processes is key to improving current and future drought representation and, thus, drought prediction and management tools.

Land-surface models (LSMs) explicitly simulate the water and energy exchanges at the interface of the soil with vegetation and the atmosphere. Compared with satellite data, the great advantage of these models is that they allow for long-term simulations that extend several decades into the past and offer a coherent image of the entire system, including variables that are difficult or impossible to observe from space, such as root zone soil moisture. LSMs are complex, which limits their use as hydrological models for daily basin management, where simple hydrological models offer better results in terms of streamflow simulation. However, because they are physical models, LSMs simulate most of the processes related to the propagation of drought through the system (Vidal et al., 2010b); thus, they are ideal for the study of processes related to drought. Furthermore, LSMs play an important role in drought prediction systems (Thober et al., 2015).

LSMs can be useful for drought monitoring and providing information regarding decision making (Sheffield and Wood, 2007; 2014). One caveat is that LSMs simulating soil moisture and its variability are affected by uncertainties in the forcing data, model structure (Koster et al., 2009; Van Loon et al., 2012), parameters (Nearing et al., 2016) and resolution; as a consequence, uncertainties are still relevant (Yilmaz and Crow 2013; Wang et al., 2009; Fan et al., 2011; Tallaksen and Stahl, 2014) and, thus, the use of ensembles in different models is recommended (Mo and Lettenmaier, 2014). The assimilation of satellite soil moisture is also a possible way to reduce uncertainty (Lopez et al., 2016), but validation with satellite data is not always straightforward (Escorihuela and Quintana-Seguí, 2016).

Regional climate models (RCMs) can help in this task. One of their greatest advantages is their adaptation to the regional scale (Feser et al., 2011). This allows us to use regional observations and to increase the model's physical parametrization complexity. Such models are suitable for drought analyses performed at the scale of large river basins. Another important aspect of RCMs is that these models are used to develop regional climate change scenarios via downscaling processes (JiménezGuerrero et al., 2013). In addition, using high resolution permits RCMs to be used to perform studies of atmospheric phenomena at a small scale. However, drought is difficult to model, as complex interactions between atmospheric and continental surface processes must be combined with human action (Van Loon et al., 2012a). Furthermore, the relationships among drought types add complexity to such modelling.

In this study, we use different land-surface models forced by three forcing datasets at different resolutions in order to

1. evaluate the usefulness of land-surface models as tools to provide drought information (e.g., precipitation, soil moisture and streamflow);
2. to analyse how RCMs characterize meteorological, soil moisture, and hydrological drought;
3. to analyse how LSMs and RCMs represent the propagation from a precipitation anomaly to a soil moisture and streamflow anomaly.
4. evaluate the involved uncertainties;
5. detect areas of improvement in land-surface modeling.

This report is based on the results published in two papers produced within this project: Barella-Ortiz and Quintana-Seguí (2019) and Quintana-Seguí et al. (2020).

2. Study area

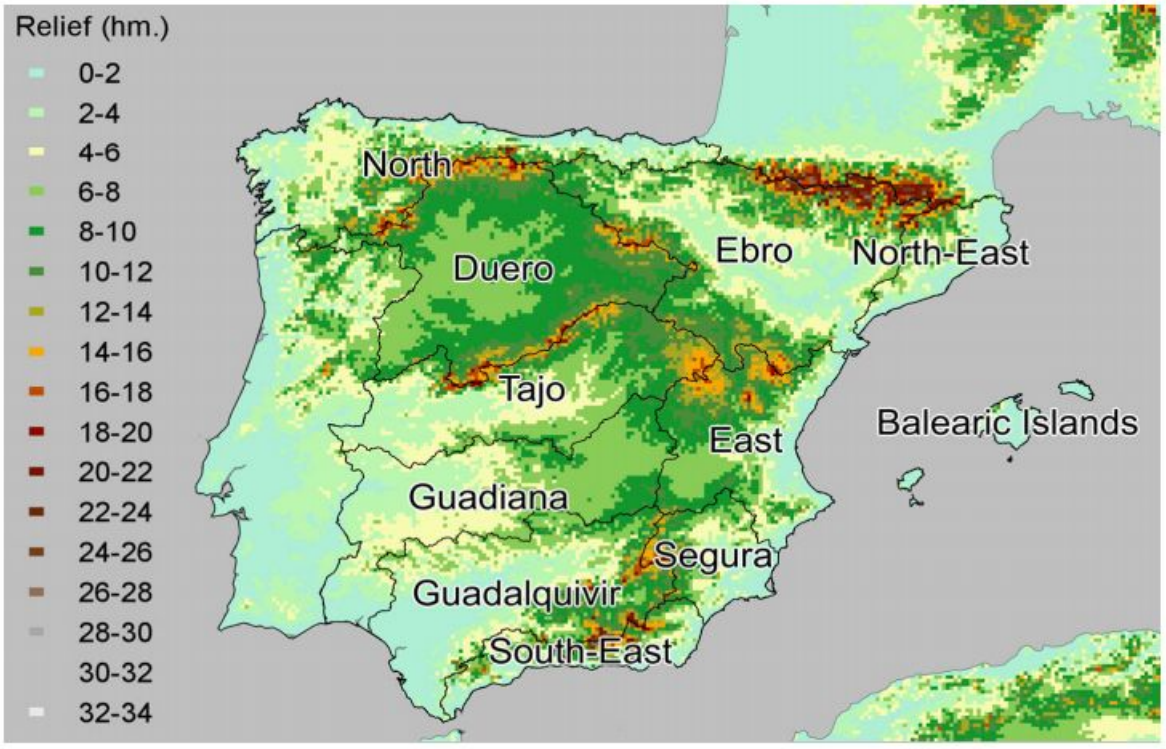

Figure 2.1. Relief and main river basins of Spain. The major rivers (Ebro, Duero, Tajo, Guadiana and Guadalquivir) are shown with their true borders; other smaller basins have been grouped in larger units (North, North-East, East, South-East and Balearic islands)

This study is focused on mainland Spain, whose relief and main basins are depicted in Fig. 2.1. The main climatic regimes of Spain are oceanic and Mediterranean. However, a semiarid climate or even a desert-like climate can be identified in the southeast (Aemet, 2011). Spain is influenced by both Atlantic (dominated by synoptic-scale frontal systems) and Mediterranean meteorology (where mesoscale convective systems are common and

often missed by global-scale and low-resolution reanalyses and datasets) which, together with complex orography, are the main factors that modulate the climate in this area. Spain has an heterogeneous distribution of the annual mean precipitation, with values ranging from 2000 mm y−1 in the Atlantic margin and Pyrenees to less than 100 mm y−1 in the SE. The main valleys, such as the Ebro basin, are dry due to the shadowing effect of the mountains. Runoff is mainly generated on the relief surrounding the main basins. Spain is known to experience frequent droughts (Olcina, 2001). In general, Spain is a semiarid region and is not densely vegetated. As a result, soil moisture displays a large annual cycle. From a hydrological point of view, there is a strong dependence of the main rivers on the precipitation generated in the nearby relief and the resulting runoff. An example is in the Ebro Basin and the Pyrenees. Agriculture is located in downstream areas, and the infrastructure has been built to store water (dams) and distribute it to irrigated fields (canals). As a result, the streamflow is significantly influenced by water management. The impact of the anthropic effect must be taken into account. According to Sousa et al. (2011), drought in Spain has increased in severity and frequency. Although precipitation does not show significant annual trends, observations show a reduction in spring and summer (de Luis et al., 2010) as well as an increase in the number of consecutive dry days (Turco and Llasat, 2011). Both aspects have an impact on soil moisture drought, which is also affected by an increase in annual and seasonal temperatures (del Rio et al., 2011; Kenawy et al., 2013). This rise in temperature increases the atmospheric demand (Vicente-Serrano et al., 2014) and thus evapotranspiration, reducing the soil's water content. For hydrological drought, we must also consider the advance in the thaw date and a thinning of the blanket of snow in mountainous areas, such as in the Pyrenees (Morán-Tejeda et al., 2013), which affect streamflow and increase this type of drought. However, it should be noted that snow melt can affect streamflow and thus hydrological drought in different ways depending on its timing (Van Loon et al., 2010).

3. Datasets and models

3.1. Atmospheric forcing datasets for offline simulations

Off-line land-surface model simulations are performed by driving the LSM with a forcing dataset. In this study, our reference dataset is SAFRAN. Furthermore, two other global and lower resolution datasets are used: the forcing dataset of the EU-FP7 eartH2Observe project and MSWEP. SAFRAN (Durand et al., 1993; 1999) is a meteorological analysis system that produces gridded datasets of screen-level meteorological variables by combining the outputs of a meteorological model and all available observations using an optimal interpolation algorithm (OI) (Gandin, 1966). SAFRAN has been extensively used in France (Quintana-Segui et al., 2008; Vidal et al., 2010a) and, more recently, it has also been applied in Spain by Quintana-Seguí, et al. (2016, 2017). The Spanish application of SAFRAN uses observational data from the Spanish State Meteorological Agency (AEMET) and ERA-Interim (Dee et al., 2011) as the first guess. The resulting gridded product has a resolution of 5km but, for this study, we have also generated a lower resolution dataset (30km). We have labeled these products as SFR (SAFRAN) and SLR (SAFRAN Low

Resolution), respectively. The high-resolution SAFRAN data used in this study are available in the HyMeX database. The EU-FP7 eartH2Observe project has produced a global reanalysis of water resources by performing global off-line simulations based on hydrological and land-surface models. These simulations need a global meteorological forcing dataset, and the project has created its own based on ERA-Interim (Dee et al., 2011). The first version of this reanalysis, which has a resolution of 0.5 degrees, is described in Schellekens et al. (2017). eartH2Observe also produced a 0.25 degree forcing dataset, which is the one we used here. It is directly derived from the original ERA-Interim 3-hourly data driving ERA-Interim/Land (Balsamo et al., 2012). Hereafter, this forcing dataset is labeled as E2O. Simulations have also been performed using E2O by substituting its precipitation dataset with the MSWEP precipitation dataset (Beck et al., 2017), which optimally merges the highest quality data sources available as a function of timescale and location. From now on, this dataset is labeled as MSW.

3.2. Land-surface models

This study is based on simulations performed with three land-surface models: SASER, LEAFHYDRO and ORCHIDEE. These incorporate a river routing scheme to transform the generated runoff into streamflow. None of the models simulate human processes, such as irrigation or dams. LEAFHYDRO includes a dynamic water table coupled via two-way fluxes into soil-vegetation and rivers.

3.2.1. SASER

SASER (SAfran-Surfex-Eaudysee-Rapid) is a hydrometeorological modeling platform based on the SURFEX land-surface model. Usually, SASER uses SAFRAN as the forcing dataset but, in this paper, it can use any other suitable dataset. SURFEX (SURFace EXternalisee) is Météo France's surface modeling platform (Masson et al. 2013). For natural soils, SURFEX uses the ISBA (Interaction Sol-Biosphere-Atmosphère) land surface scheme (Noilhan and Planton, 1989; Noilhan and Mahfouf, 1996), which has different versions. In this study, we have selected ISBA-3L (Boone et al., 1999) and ISBA-DIF (Boone, 2000; Habets et al., 2003). The former considers a simple three-layer description of the soil by means of a force restore approach, while the latter uses a more complex multilayer approach. SURFEX lacks a routing scheme, which is the reason why SASER uses the RAPID routing model (David et al., 2011a, b). The connection between SURFEX and RAPID is made by means of Eau-dysee. An important limitation of SASER is that it does not represent groundwater processes. In this study, SURFEX has been run on the same grid as SAFRAN, which has a resolution of 5km. Simulations have been performed using ISBA-DIF and ISBA-3L. Hereafter, the SURFEX simulations that use ISBA-DIF are labeled as DIF, and the SURFEX simulations that use ISBA-3L are labeled as 3L.

3.2.2. LEAFHYDRO

LEAF (Land-Ecosystem-Atmosphere Feedback) is the land-surface component of RAMS (Regional Atmosphere Modeling System) (Walko et al., 2000). Several modifications were made to LEAF to incorporate groundwater processes, resulting in LEAFHYDRO (Miguez-Macho et al., 2007). The water table depth is diagnosed based on the soil moisture when it lies within the resolved soil layers. When the depth is deeper, soil columns are extended to the dynamic water table below, thereby acting as saturation boundary conditions and affecting the soil water fluxes above. There is lateral groundwater flow among adjacent cells, leading to divergence from the high ground and convergence with low valleys at multiple scales. The water table, once recharged by rain events or fed by lateral flow convergence,relaxes into rivers within a grid cell through fluxes between groundwater and rivers. These fluxes can be 2-way depending on the hydraulic gradient, representing both loosing (i.e., leaking into groundwater) and gaining (i.e., receiving groundwater) streams. River discharge, which is fed by surface runoff and groundwater, is routed out to the ocean through the channel network using the kinematic wave method. The sea level is set as the head boundary condition for groundwater, which allows it to influence coastal drainage.

The LEAFHYDRO simulations for this study were performed on a grid with a 2.5 km resolution that is nested in the 5 km SAFRAN grid, which allows each cell in the SAFRAN grid to exactly encompass 4 cells of the LEAFHYDRO grid. Afterwards, the results were aggregated to 5 km to facilitate the comparisons with the SASER-based simulations. Hereafter, LEAFHYDRO is labeled as LHD.

3.2.3. ORCHIDEE

The ORCHIDEE LSM (De Rosnay and Polcher, 1998; Krinner et al., 2005) was developed by the Institut PierreSimon Laplace (IPSL). It can be run in a stand-alone mode or coupled to the Laboratoire de Météorologie Dynamique (LMD-Z) general circulation model (Li, 1999), which was developed by the LMD in Paris. Hydrology is approached by means of a diffusive equation with a multilayer scheme. For this, the Fokker–Planck equation is solved considering a soil depth of 2 m distributed across 11 layers. The fine resolution is key to better model the interaction between the root profile and the soil moisture distribution at different depths as well as infiltration processes. In addition, ORCHIDEE includes sub-grid variability in soil moisture. Each grid box is divided into three soil moisture profiles with different vegetation distributions, but the same soil texture and structure that are obtained from the Zobler map (Post and Zobler, 2000).

3.3. Regional Climate Models

In this study, drought representation and propagation in three RCMs are analysed. RCM simulations were downloaded from the Med-CORDEX database, which is a contribution to the Coordinated Regional Climate Downscaling Experiment (CORDEX, Giorgi et al., 2009) focusing on the Mediterranean region (Ruti et al., 2016). The criterion used to select the

models was that each one used a different surface scheme and therefore represented physical processes related to precipitation, soil moisture, and surface and sub-surface runoff in different ways. The three RCMs selected are listed in Table 1 and described below:

- The CNRM-RCSM4 (Sevault et al., 2014; Nabat et al., 2014) is a RCM developed by the CNRM. It includes the regional climatic atmospheric model "Aire Limitée Adaptation dynamique Développement InterNational" (ALADIN-Climate, Radu et al., 2008; Déqué and Somot, 2008; Farda et al., 2010; Colin et al., 2010; Herrmann et al., 2011), the three-layer version of the ISBA LSM (Noilhan and Planton, 1989; Noilhan and Mahfouf, 1996), the Total Runoff Integrating Pathways (TRIP) routing scheme (Decharme et al., 2010), and the regional ocean model NEMOMED8 (Beuvier et al., 2010). Hereafter, it will be referred to as RS4.
- The COSMO-CLM (CCLM) model (Rockel et al., 2008) is the climate version of the COSMO model developed by the Goethe Universität Frankfurt (GUF). The surface scheme is a multilayer version of the Jacobsen and Heise (1982) two-layer model. Hereafter, it will be referred to as CL4.
- The PROMES model (Castro et al., 1993; Sánchez et al., 2004; Domínguez et al., 2010) was developed by the Universidad Complutense de Madrid (UCM) and the Universidad de Castilla-La Mancha (UCLM). It is coupled to the ORCHIDEE LSM (De Rosnay and Polcher, 1998; Krinner et al., 2005). Hereafter, it will be referred to as PMS.

All of the RCM simulations are driven by the ECMWF Interim reanalysis (ERA-Interim) (Balsamo et al., 2012; Dee et al., 2011), which provides a global atmospheric reanalysis that starts in 1979 and is continuously updated in real time. In addition, it improves some important issues pertaining to ERA-40, such as the representation of the hydrological cycle. This reanalysis is performed by means of a data assimilation system based on a 2006 release of the ECMWF's Integrated Forecast System, IFS (Cy31r2), and uses a four-dimensional variational analysis (4D-Var) with a 12 h analysis window. The database has atmospheric and surface parameters with a temporal scale of 6 and 3 h, respectively. The spatial resolution is 80 km, with 60 vertical levels from the surface to 0.1 hPa

ERA-Interim is a well-known atmospheric forcing used in a large number of studies. For instance, Belo-Pereira et al. (2011) and Quintana-Seguí et al. (2017) have validated it across the Iberian Peninsula. However, biases in this type of forcing have a negative effect on LSM simulations, which can be corrected (Ngo-Duc et al., 2005; Weedon et al., 2011).

In this study, ERA-Interim is the driving data of the three RCMs analysed. In addition, it is also used to force LSM simulations used as a reference in the soil moisture drought analysis. Hereafter, it will be referred to as ERA.

For the hydrological drought analysis, modelled and observed streamflow data were used as references. Two issues should be stressed before explaining these datasets. The first is that the Med-CORDEX database does not provide simulated streamflow for any of the three RCMs, which would be the variable ideally suited for this study. In the absence of such data, it was decided to use modelled total runoff (hereafter referred to as runoff) corresponding to the subbasins defined by a selection of gauging stations. We believe that this approximation

is valid because we use a coarse time step, with a larger time propagation than the flow propagation. In fact, other studies use this variable to analyse hydrological drought (Vu et al., 2015; Meresa et al., 2016).

3.4. Streamflow observations

Daily streamflow data were obtained from the MAPAMA database. To obtain monthly time series with few gaps, we selected all stations that had at least 95% of the daily data during the period of study.

Due to the high degree of human influence on streamflow in the area of study, an estimate of the monthly naturalized flow was necessary in order to validate our LSM simulations, which do not simulate any water management infrastructure. SIMPA (Estrela and Quintas, 1996; Ruiz 1999) is a monthly, conceptual, distributed hydrological model used by MAPAMA and the authorities of most basins, which provide feedback during its development. We believe that it is currently the best reference dataset for naturalized flow for Spain. These data were provided to us by MAPAMA. Its streamflow time series ends in summer 2006. Hereafter, SIMPA is also referred to as SMP.

4. Methodology

4.1. LSM simulations

The offline LSM simulations performed in this study encompass the period 1980-2013; however, all calculations based on streamflow have been performed in the subperiod (1982-2005). This was done for two reasons: (1) the SMP time series provided by the MAPAMA ends in summer 2006; and (2) in the LHD simulations, due to the spin-up process, the simulated streamflow was not realistic until 1982.

To compare the simulated soil moisture among models, soil was divided into two layers: the root zone and deeper soil zone. SURFEX defines the root zone and deeper soil zone coherently in both 3L and DIF. To do the same in LHD, we used the root zone and total soil depth of 3L and then extracted the soil moisture for these same layers in LHD.

4.2. Drought quantification

4.2.1. Calculation of drought indices

We have calculated drought indices following the SPI. This index is calculated using monthly data or, alternatively, a time series of the accumulated precipitation for the previous n months, where n represents the scale of the index. A similar operation can be done for soil moisture (SSMI) and streamflow (SSI). We use a nonparametric methodology, which can be

applied to different climatic variables, including precipitation, soil moisture and relative humidity, without having to assume representative parametric distributions (Farahmand and AghaKouchak 2015).

4.2.2. Drought propagation

The methodology we used to study drought propagation is inspired by Barker et al. (2015): (1) the standardize soil moisture index (SSMI) is calculated with a temporal accumulation of 1 month, making the SSMI equivalent to SSMI-1; (2) for precipitation, SPI-n is computed for n in [1, 2, ..., 24]; and (3) finally, for any given grid point, the nx scale maximizing the Pearson correlation coefficient between SPI-n and SSMI is found. The resulting nx can be interpreted as the scale at which drought propagates from precipitation anomalies to soil moisture anomalies. For streamflow, the methodology is mostly the same, with the difference being that the SPI is calculated with the areal mean of the basin precipitation corresponding to the gauging station of the studied streamflow.

4.2.3. Comparison and validation metrics.

To compare standardized indices of the same variable (i.e. soil moisture) corresponding to two different products or to a product and the observations we have used the root mean square difference (RMSD) and Pearson Correlation coefficient (r).

The streamflow validation was carried out using the Kling– Gupta efficiency (KGE) (Gupta et al., 2009). The optimal KGE value is 1, whereas negative values are a sign of a model's bad performance.

5. Results

5.1. Meteorological drought

5.1.1. Mean annual precipitation

Fig. 5.1.1.1 shows the mean annual precipitation in the area of study, as reproduced by the forcing datasets used in this study. SFR (a), our reference dataset, captures the complexity of the spatial structure of precipitation in Spain. The most important factors determining its distribution are relief (increased precipitation in the main mountain ranges due to orographic lift enhancement and a decrease in inland valleys, due to rain shadowing effect) and the proximity to the Atlantic ocean, upwind from the prevailing westerly flow. SLR (c) is a lower resolution version (30km) of SFR, with a smoother spatial structure retaining nonetheless its main patterns and features. The difference between both datasets (b) shows the error due to resolution and, as expected, is largest on the relief. SLR is similar in resolution to E2O and

MSW, thereby allowing for a fairer comparison than SFR. E2O (d) resolves less features in the precipitation pattern than SLR (and hence, SFR), and presents a strong negative bias (e) in most of the area of study. The exceptions are concentrated in the inland valleys of the Ebro and the Duero basins, where precipitation is overestimated due to the misrepresentation of the shadowing effect of the relief by E2O. MSW (f) , also overestimates precipitation (f), but to a lesser degree than E2O, which attests to the incorporation of other sources of precipitation information (from satellite, rain gauges, etc.) representing an important improvement. Notwithstanding, MSW still overestimates precipitation in the Ebro valley (but not in the Duero) and also in a small area of the South East. These results are in accordance with those found by Belo-Pereira et al (2011), who validated the precipitation of different global datasets in the Iberian peninsula.

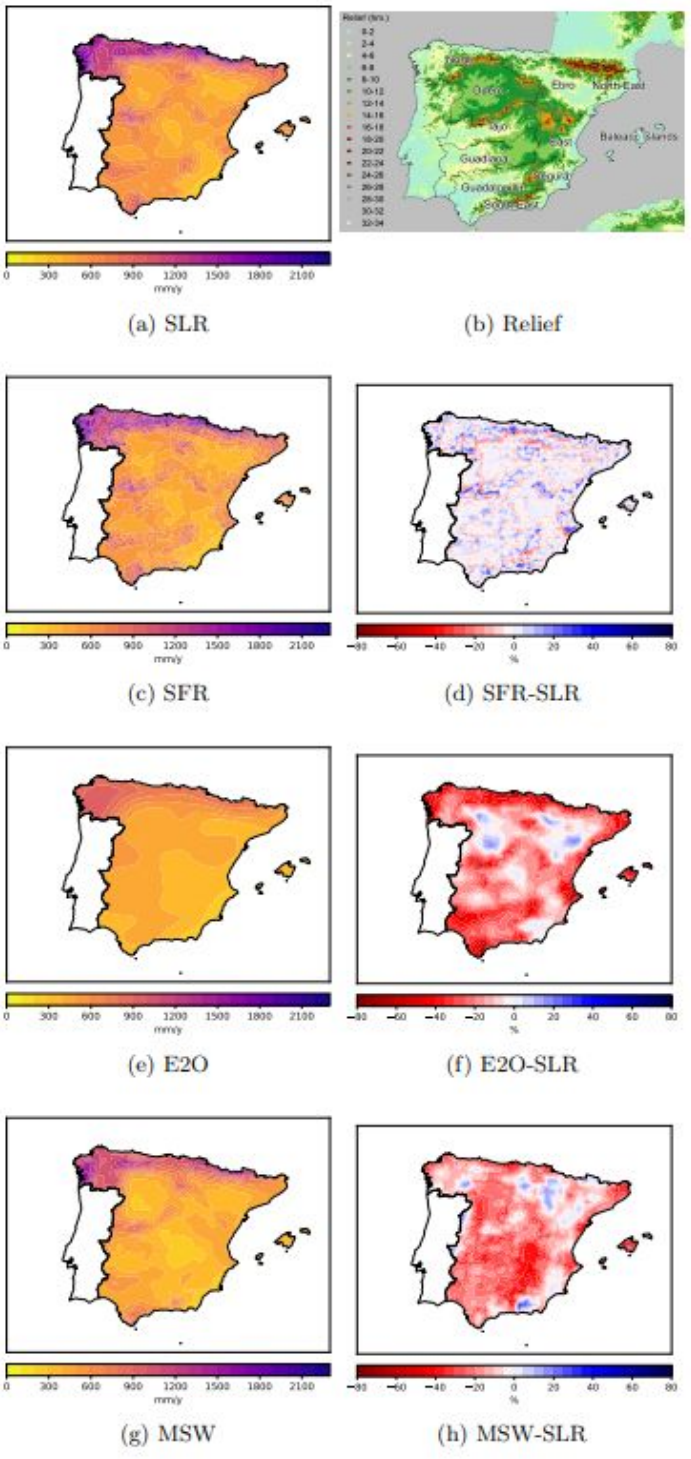

Fig. 5.1.1.1. Mean annual precipitation of the forcing datasets in the area of study for the period 1980-2013 from the four products used in this study. Panel (b) shows the relief at the resolution of the SFR grid (5 km) and the main river basins (small ones have been aggregated). All products have been regridded to the SFR grid, which is the one used in the LSM simulations. The first column shows means and the second column, differences using SLR as reference.

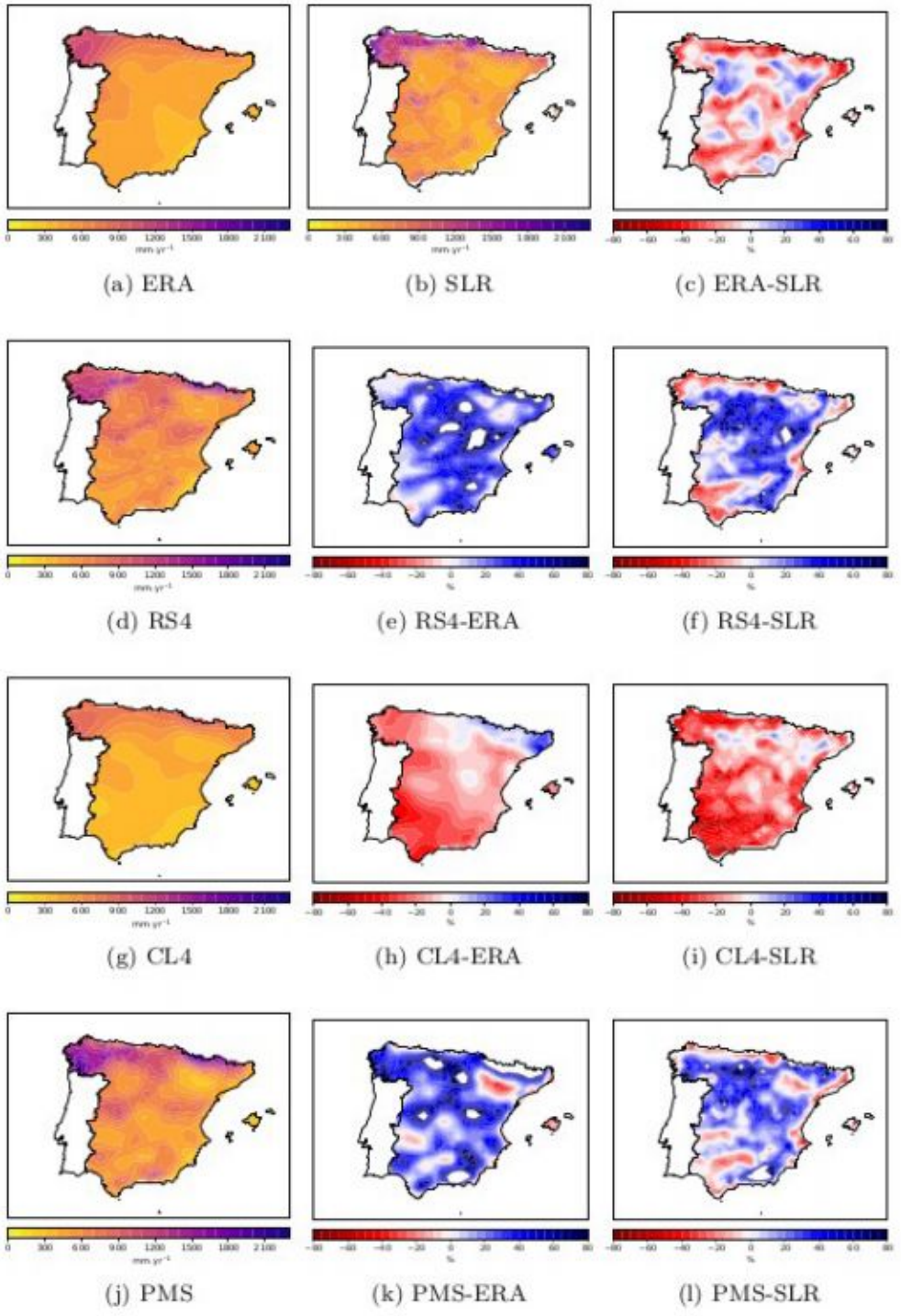

Fig 5.1.1.2. Mean annual precipitation of the RCMs across the study area from 1989 to 2008: ERA (a), SLR (b), RS4 (d), CL4 (g), and PMS (j). Panel (c) shows the difference between ERA and SLR mean annual precipitation; panels (e), (h), and (k) show the difference between the RCMs and ERA mean annual precipitation; and panels (f), (i), and (l) show the difference between the RCMs and SLR mean annual precipitation.

Figure 5.1.1.2. shows the mean annual precipitation of ERA and SLR as well as the difference in mean annual precipitation between them. Panels d–l show the RCMs' mean annual precipitation and their difference with respect to ERA (Panels e, h and k) and SLR (Panels f, i, l). All products show greater precipitation in the northwestern and northern regions of the peninsula (exceeding 2000 mm yr−1) as well as over mountainous chains. The products also show that precipitation is lower along the main basin valleys (due to the orographic shadow effect) and minimal over the southeast, which is the driest region of the peninsula. For instance, precipitation across some areas of this region does not exceed 100 mm yr−1 . The RCMs' mean precipitation spatial structures show similar behaviour to those from ERA and SLR. The fact that precipitation is high over mountainous chains indicates the strong influence of relief, which is key in the way water from precipitation is distributed. In fact, we would like to stress SLR's significant contrast in relief due to its use of data from AEMET's dense pluviometric network. This evidence indicates the complex spatial structure of precipitation in Spain.

Regarding the RCMs, RS4 and PMS show the greatest similarity and the highest contrast with CL4. When compared to ERA, both RCMs have higher precipitation, especially in mountainous areas. Modelled precipitation tends to overestimate precipitation compared with observations and ERA (Sylla et al., 2010). This reflects the addition of water in the form of precipitation, improving the RCMs' spatial distribution of precipitation with respect to the driving data. However, when RS4 and PMS are compared to SLR, precipitation is underestimated over some areas (valleys and the coastline). It must be noted that SAFRAN is mainly based on rain gauge information. The CL4 model is a different matter, as it underestimates precipitation for almost all of Spain when compared with ERA and SLR.

5.1.2. Precipitation Drought Indices

In the previous section we found something that was expected, as it is well known that global products underestimate precipitation, especially on the relief. However, in the context of this study, it is more interesting to study the variability of the products, that is, their capacity to reproduce drought. This is the objective of this section. Figure 5.1.2.1 shows time series of SPI-12 computed from area averaged precipitation over Spain. SPI-12 from SFR, our reference dataset (Panel a) indicates that several drought events have occurred during the period, the most severe in 2004-2005. These drought spells coincide with those detected, for instance, by Belo-Pereira et al (2011). Panels (b) and (c) show the same index estimated from E2O and MSW data, respectively (we should not forget that MSW integrates rain gauge data, when comparing these two products). At first sight, the time series look similar, with the main drought periods well detected by the different products. However, there are relevant differences in both drought duration and intensity. This is better seen in panels (e) and (f), which depict the differences between E2O and SFR and MSW and SFR, respectively The differences between E2O and SFR present a noticeable trend, which can affect drought studies, as it modifies the intensity of droughts with time. To determine whether this trend develops from the original ERA-Interim data (ERA from now on), on which E2O is based, or it is due to corrections applied by the algorithms used to produce E2O, panel (d) shows the difference between ERA and SFR. The plot reveals that the problem is mainly inherited from ERA. For MSW (f) the differences with SFR are smaller, which means that the MSW

algorithm effectively combines diverse sources of data, including ERA, other reanalyses, satellite and rain gauge observations, in order to better estimate real precipitation. However, even when the differences are reduced in this case, they remain relevant. An analysis of the monthly maps of drought for the three products (not shown) reveals that E2O and MSW are able to reproduce the main drought spatial patterns, but miss the finer details. MSW is nevertheless an important improvement compared with E2O. If we study the time evolution of the spatial correlation (not shown) we see that MSW has better correlations and less variability in time (more robustness) than E2O, which sometimes completely misses the spatial structure of drought, with very low correlations that approach zero for some months. Looking at the evolution of the area under drought (not shown) the errors of SLR are minimal, but still reaching 6% for some months. MSW does not present a systematic bias, but it overestimates the area under drought in the first part of the 1990s and it underestimates it from year 2006 on. E2O shows the trend seen before (increasing drought with time). In addition, we have also studied the temporal correlation of the drought indices for each grid point. As the most interesting result, this comparison denotes the improvement that MSW represents with respect to E2O. E2O has lower correlations in the Ebro basin and the Mediterranean coast, which is a known limitation of global products in the Iberian Peninsula (Belo-Pereira et al., 2011; Andrade and Belo-Pereira, 2015). The incorporation of satellite rainfall data into MSW ameliorates the detection of the small scale structures that produce precipitation in the Mediterranean area. SLR has high temporal correlations with SFR, as expected.

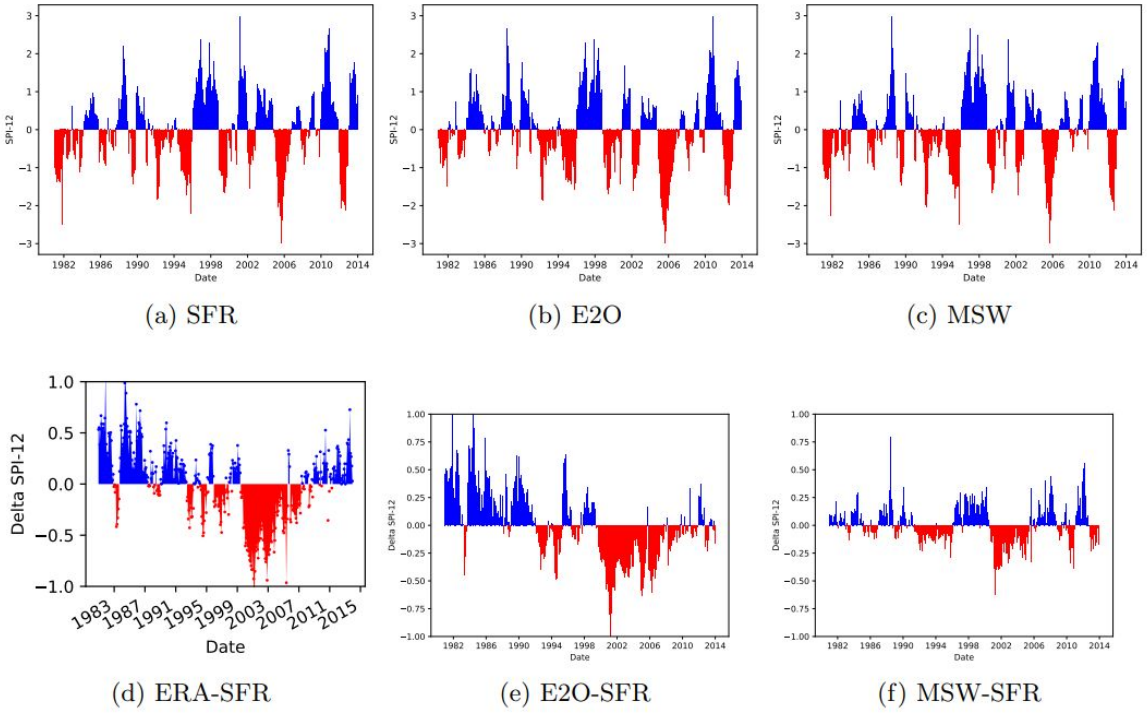

Figure 5.1.2.1. SPI-12 time series. First row: SPI-12 calculated with the spatially aggregated time series of precipitation of Spain as reproduced by SFR, E2O and MSW. Second row: Difference between the aggregated SPI-12 time series calculated with ERA, MSE and E2O compared to SFR.

Figure *5.1.2.2.* shows the time series of the SPI-12 calculated using mainland Spain's average precipitation as reproduced by ERA (panel a), SLR (panel b), and the RCMs (panels d, g, and j). The computation is performed for a time accumulation of 12 months. ERA and SLR show several drought spells which occurred during the 20 years that comprise the study period (the most severe occurred in 2005–2006). These spells coincide with those found by Belo-Pereira et al. (2011) and also appear in the RCMs' SPI time series plots. Therefore, RCMs are capable of reproducing these spells. However, differences in duration and severity can be observed. For instance, the duration of the spell that occurred in 1992 and 1993 was 21 and 22 months according to CL4 and PMS, respectively. However, it lasted 19 and 17 months according to SLR and ERA, respectively. Another interesting result is found in the spell that took place in 2002. CL4's mean severity is similar to that of ERA. However, the mean severity of both RS4 and PMS is in better agreement with that of SLR than with their driving data. Other information that can be extracted from these results is the timing of drought between the RCMs and their driving data and reference data. For example, the RCMs, ERA, and SLR agree that the spell that occurred between 1994 and 1995 started in May 1994. RS4, CL4, ERA, and SLR agree that it ended in December 1995, but the PMS model indicates the end of the spell occurred a month before the rest (November 1995). The spell between 2004 and 2006 started in November 2004 according to SLR, ERA, and PMS, which show similar durations (ERA shows 23 months, and SLR and CL4 show 24 months). However, it started in January 2005 according to RS4 and CL4 and had a longer duration:

27 (RS4) and 25 (CL4) months. In a previous study, a spurious trend in ERA was detected (QuintanaSeguí et al., 2019). This can be observed in Panel d, where the difference between the SPI-12 time series of ERA and SLR is represented. However, the differences between the RCMs and SLR SPI-12 time series show that these models do not drag this trend.

To deepen the analysis of the spatial structure of meteorological drought, monthly SPI-12 maps were computed. The comparison of these structures, as shown by the RCMs, with those of their driving data and the reference dataset, provides more information about drought representation by RCMs. For instance, the temporal evolution of the spatial correlation of the SPI-12 maps of the RCMs with ERA and SLR (not shown) indicates the similarity between the RCMs and their driving data and reality (as approximated by SLR), respectively. In the first case, RS4 most resembles ERA. Despite not showing the highest correlations, it has less variability and is therefore more robust. The correlations of CL4 and PMS with ERA are more variable, reaching values close to zero in some months, in which the spatial structure of drought is not captured. In the second case, RCMs show worse correlation with SLR than with ERA, as expected. It should be stressed that RS4 also displays better correlations than the other RCMs when these are compared with SLR. Thus, out of the three RCMs studied, RS4 deviates less from the driving data and most resembles the reference. The correlation between ERA and SLR shows some variability in its temporal evolution, especially since 2000. This is likely due to the effect of the spurious trend identified previously. To complement the spatial structure analysis, we look at the difference in the percentage of the area affected by drought (SPI-12 < −1) between the RCMs and ERA and SLR (not shown). The differences are generally under 25 %. In general, the RCMs show similar behaviour during a drought spell, meaning that they all overestimate or underestimate the affected area. For example, all three underestimate the area in 1994, overestimate it in 1995, and underestimate it in 1996. The difference relates to the degree to which they deviate. On the one hand, in 1995, RS4 overestimates the percentage of area affected by drought by 20 %, CL4 by approximately 15 %, and PMS by less than 10 %. On the other hand, in 1996, PMS underestimates this percentage by more than 30 %, while RS4 and CL4 underestimate it by 10 %. Another example is how the RCMs overestimate the area in 2000 and how they underestimate it between 2001 and 2003. RS4 is the RCM that shows the lowest percentage difference, which is consistent with our previous results.

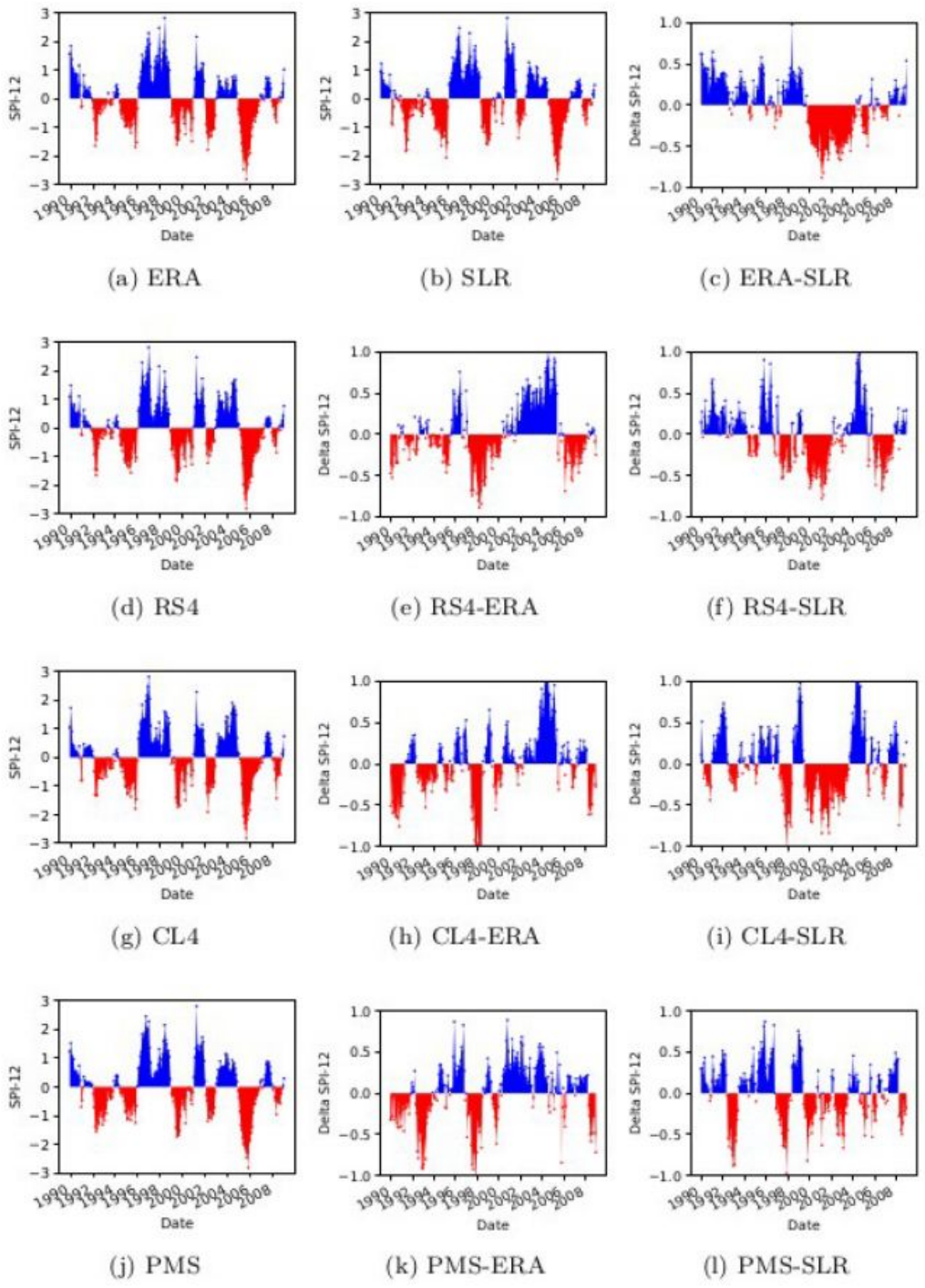

Figure 5.1.2.2. SPI-12 time series calculated with the spatially averaged time series of mainland Spain precipitation, as reproduced by ERA (a), SLR (b), RS4 (d), CL4 (g), and PMS (j). Panel (c) shows the difference between ERA and SLR SPI-12; panels (e), (h), and (k) show the difference between the RCMs and ERA SPI-12; and panels (f), (i), and (l) show the difference between the RCMs and SLR SPI-12.

5.2. Soil Moisture Drought

5.2.1. Soil Moisture Drought Indices

In this section, we quantify the model result differences and assess the intermodel consistency for soil moisture drought. Table *5.2.1.1.* shows the root mean square difference (RMSD) and Pearson correlation (r) calculated by comparing all simulations with each other. These values synthesize both the spatial and temporal aspects of the differences, as the comparisons include all data points (i.e., all grid points for all time steps). The table contains four subtables. The first row of subtables corresponds to the root zone, and the second row corresponds to the deep soil. Different color scales have been used for each score (RMSD and r), but the same color scale (where greener is better) is used for each score for both soil layers.

Root zone

RMSD	E2O-DIF	E2O-LHD	MSW-DIF	MSW-LHD	SLR-DIF	SFR-DIF	SFR-LHD	SFR-3L
E2O-DIF		0,54	0,49	0,66	0,57	0,61	0,73	0,68
E2O-LHD			0,67	0,52	0,71	0,74	0,61	0,7
MSW-DIF				0,54	0,42	0,48	0,64	0,58
MSW-LHD					0,61	0,65	0,47	0,6
SLR-DIF						0,28	0,56	0,47
SFR-DIF							0,55	0,42
SFR-LHD								0,46
SFR-3L								

r	E2O-DIF	E2O-LHD	MSW-DIF	MSW-LHD	SLR-DIF	SFR-DIF	SFR-LHD	SFR-3L
E2O-DIF		0,85	0,88	0,77	0,83	0,8	0,72	0,76
E2O-LHD			0,76	0,86	0,73	0,71	0,8	0,74
MSW-DIF				0,85	0,91	0,88	0,78	0,82
MSW-LHD					0,8	0,78	0,88	0,81
SLR-DIF						0,96	0,83	0,88
SFR-DIF							0,84	0,9
SFR-LHD								0,89
SFR-3L								

Deep soil

RMSD	E2O-DIF	E2O-LHD	MSW-DIF	MSW-LHD	SLR-DIF	SFR-DIF	SFR-LHD	SFR-3L
E2O-DIF		0,69	0,54	0,83	0,65	0,7	0,89	0,96
E2O-LHD			0,75	0,53	0,76	0,79	0,63	0,73
MSW-DIF				0,69	0,45	0,53	0,78	0,87
MSW-LHD					0,71	0,73	0,48	0,63
SLR-DIF						0,31	0,68	0,77
SFR-DIF							0,65	0,74
SFR-LHD								0,5
SFR-3L								

r	E2O-DIF	E2O-LHD	MSW-DIF	MSW-LHD	SLR-DIF	SFR-DIF	SFR-LHD	SFR-3L
E2O-DIF		0,75	0,85	0,63	0,78	0,74	0,58	0,51
E2O-LHD			0,7	0,85	0,69	0,67	0,79	0,72
MSW-DIF				0,74	0,89	0,85	0,68	0,6
MSW-LHD					0,74	0,72	0,88	0,79
SLR-DIF						0,95	0,76	0,68
SFR-DIF							0,78	0,71
SFR-LHD								0,87
SFR-3L								

Table 5.2.1.1. Comparison of the SSMI data produced by all simulations.

Two scores have been computed, the root mean square difference (RMSD) and the Pearson correlation (r), for the root zone SSMI and deep soil SSMI

The disparity between simulations with the same model but different forcings is larger than that between simulations with the same forcing but different models, which implies that the forcing dataset plays an important role. For example, in simulations forced by SFR, the largest RMSD for the root zone soil moisture is 0.55, and the lowest correlation is 0.84 (both

correspond to SFR-DIF vs. SFR-LHD). On the other hand, for all simulations using DIF, the largest RMSD is 0.61, and the lowest correlation is 0.80 (E2O-DIF vs. SFR-DIF). This result is identical if we compare E2O-LHD with SFR-LHD. For the root zone soil moisture, the smallest difference between two simulations that use different forcing datasets and models is between E2O-DIF and SFR-3L (RMSD = 0.42 and r = 0.9). The largest difference is between E2O-LHD and SFR-DIF (RMSD = 0.74 and r = 0.71). To put these results into context, a RMSD of 0.74 is almost 3 4 of a standard deviation, which means that the drought status of a grid point at a given time probably changes category. The trend found in E2O increases the differences between simulations. If E2O is removed from the comparison, the simulations with the largest differences are MSW-LHD and SFR-DIF (RMSD = 0.65, r = 0.78), which are still high values. For deep soil moisture, the differences are larger; the most divergent simulations (taking E2O out of the comparison) are MSW-DIF and SFR-3L (RMSD = 0.87 and r = 0.6). When including E2O, the largest difference is between E2O-DIF and SFR-3L (RMSD = 0.96 and r = 0.51). This analysis shows that drought studies performed in the same area with different models and forcing datasets should be compared carefully, as the uncertainties are still high. This is something that, for example, has also been found in a climate change setting by Marx et al. (2018).

RMSD	ERA-CL4	ERA-PMS	ERA-ORC	ERA-ISB	SLR-ISB
ERA-RS4	1.3	1.26	1	0.79	0.81
ERA-CL4		0.96	1.12	1.2	1.24
ERA-PMS			1.23	1.17	1.19
ERA-ORC				0.87	0.97
ERA-ISB					0.58

r	ERA-CL4	ERA-PMS	ERA-ORC	ERA-ISB	SLR-ISB
ERA-RS4	0.3	0.36	0.46	0.66	0.65
ERA-CL4		0.65	0.5	0.35	0.3
ERA-PMS			0.39	0.39	0.37
ERA-ORC				0.58	0.49
ERA-ISB					0.82

Table 5.2.1.2. Comparison of the SSMI data from the RCM and LSM simulations. The upper block shows the RMSD, and the lower block shows the Pearson correlation (r). The colour scale is a gradient from blue (largest similarity between models) to red (lowest similarity between models) via white.

We perform the same process for the RCMs. The RMSD and the Pearson correlation coefficient (r) are calculated by comparing the SSMI from the RCM simulations and the LSM simulations. All mesh points and time steps are included in the comparison. Therefore, the results provide information regarding spatial and temporal drought structures. It should be noted that biases are not calculated because they are zero by construction (the mean of the

SSMI is zero). The results are shown in Table *5.2.1.2*, the upper block of the table corresponds to the RMSD and the lower block corresponds to the r calculations. A colour scale consisting of a blue (largest similarity between models) to red (lowest similarity between models) gradient via white has been included to facilitate reading.

To put these results into context, we will consider the drought classification according to the SPI, which is divided into eight categories from “extremely wet” (SPI = 2) to “extreme drought” (SPI = −2). A RMSD equal to 1 is a standard deviation of the index studied (in this case, the SSMI). In the framework of drought analysis, a value higher than 0.5 would imply a change in category (for example, from “slightly wet” to “moderately dry”). Therefore, the upper block of Table 3 shows that there is a change in drought category when comparing the RCMs with the reference offline LSM simulations, as the RMSD is above 0.5 (fourth to sixth columns). In addition, the three RCMs compared among them also represent soil moisture droughts of different categories (second and third columns), as expected.

Going into detail, we can observe some similarity between the RS4 simulation, which uses the ISBA surface scheme, and the ISB simulations. Compared with ISB, RS4 reproduces drought better than the other RCMs used in this study. However, this does not occur when the PMS and ORC simulations are compared, despite using the same surface scheme. In fact, RS4 and CL4 are, in general, more similar to ORC than PMS, according to the statistics. The SSMI comparison of the RCMs with both ISB simulations (fifth column vs. sixth column) shows very similar statistics. Discrepancies could be explained by the RCMs’ land–atmosphere coupling and forcing effects.

5.2.2. Drought Propagation to Soil Moisture

If the drought status is important for a water manager, the time scales of drought propagation (from precipitation to soil moisture) are perhaps even more important, as their knowledge can be a tool for the forecasting of the soil moisture status in places where drought dynamics are relatively slow, which could benefit early warning systems. As stated in Section 4.2.2 we perform this analysis by finding the nx scale maximizing the correlation between SPI-n and SSMI.

Figure 5.2.2.1 shows maps of nx for the root-zone soil moisture. For instance, by taking SFR-DIF (a) and SFR-LHD (b), it is apparent that the spatial pattern of nx is significantly different for each model. The spatial structure in DIF is overly homogeneous, which means that for this model, the SSMI correlates better with the SPI at scales of 2 months for almost all of the study area. In contrast, the LHD presents a richer pattern, with scales that extend from 3 to 12 months, as the dynamics are slower towards the south and faster towards the northwest. 3L is similar to DIF but with a NW-SE gradient that extends from scales of 1 month in the NW to 9 months in the SE. The conclusion of this first comparison is that the model formulations have a strong influence on the temporal scale at which the variability of precipitation affects the variability in soil moisture; thus, different models yield significantly different results. Another important question is how meteorological forcing affects nx . The first column in Fig. 5.2.2.1 (panels a, d, f, and h), showing the nx results for all simulations

that use the DIF model, shows that the pattern is largely invariant. E2O-DIF and MSW-DIF have an area where nx is one month longer than that in SFR-DIF, but this difference is significantly lower than that from the changing model. The results for the LHD model (second column; panels b, e and g) indicate that the spatial patterns of nx for different forcings are more divergent than those in the case of DIF but still to a lesser degree than those of a different model. This suggests that, for some models, the forcing dataset has an impact on how precipitation variability propagates to soil moisture; however, this impact is still not as high as that of the model formulation itself.

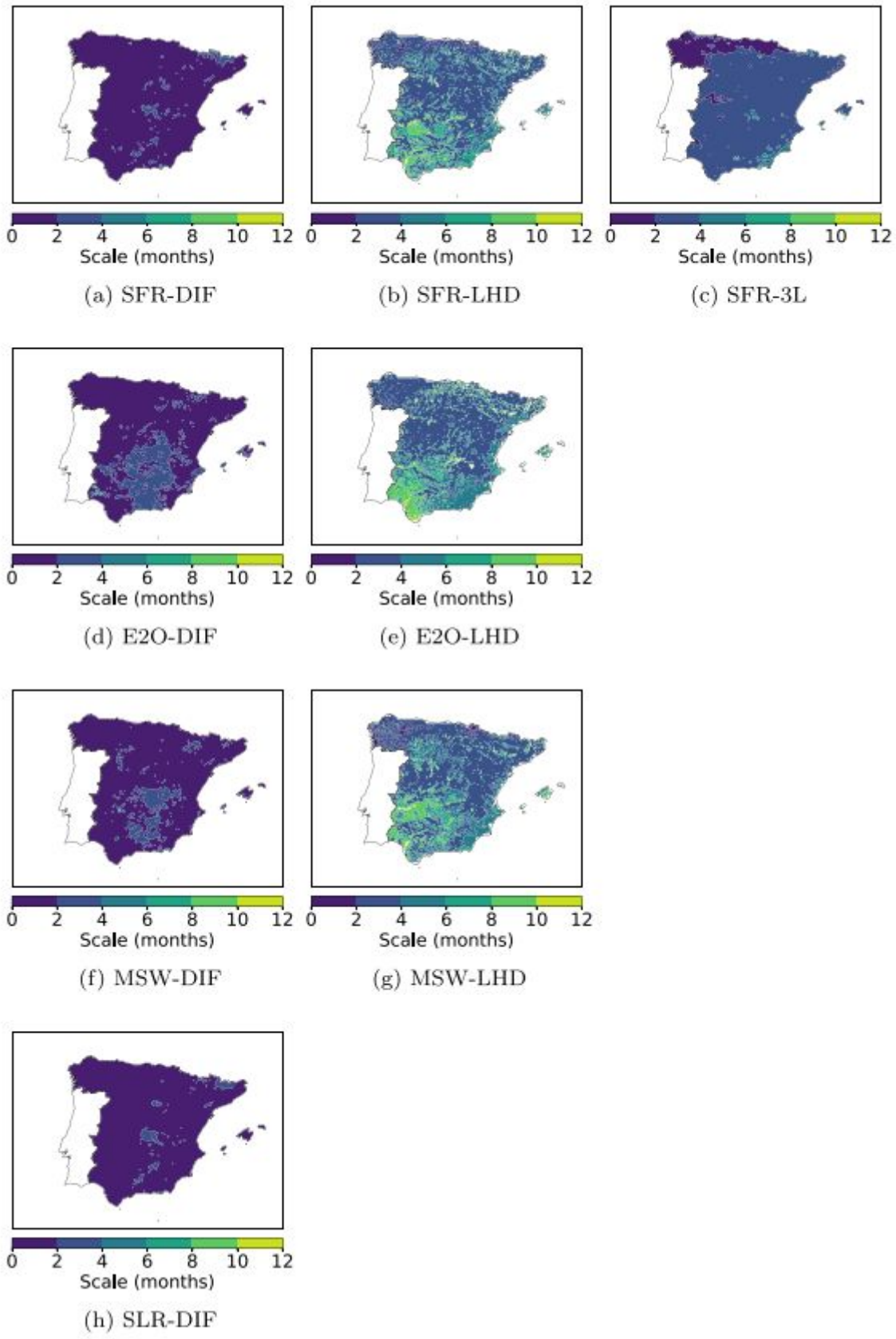

Figure 5.2.2.1. Scale nx that maximizes the correlation between SPI-n and root-zone SSMI for different forcing and model combinations.

A similar analysis can be performed for the deeper soil zone (below the root zone). In this case, (figures not shown), nx is higher for all models except 3L, indicating that soil moisture variability in the deeper soil is generally related to more persistent precipitation anomalies, which is expected. For DIF, nx is much larger in the deep soil than in the root zone when compared with the LHD results, where there is much less variation. This occurs perhaps because of the relatively fine resolution of the soil columns in the top 4 m of the soil and the coupling with the water table in this model.

These comparisons show that LSMs with different structures produce different drought dynamics in soil moisture. Unfortunately, we do not know what the reality is due to the lack of observations, but these large differences reveal that progress is needed in order to, first, improve the observational coverage of the soil moisture (particularly the deeper layers) and, second, bring models closer to the real behavior. Furthermore, the forcing dataset also introduces its own uncertainty.

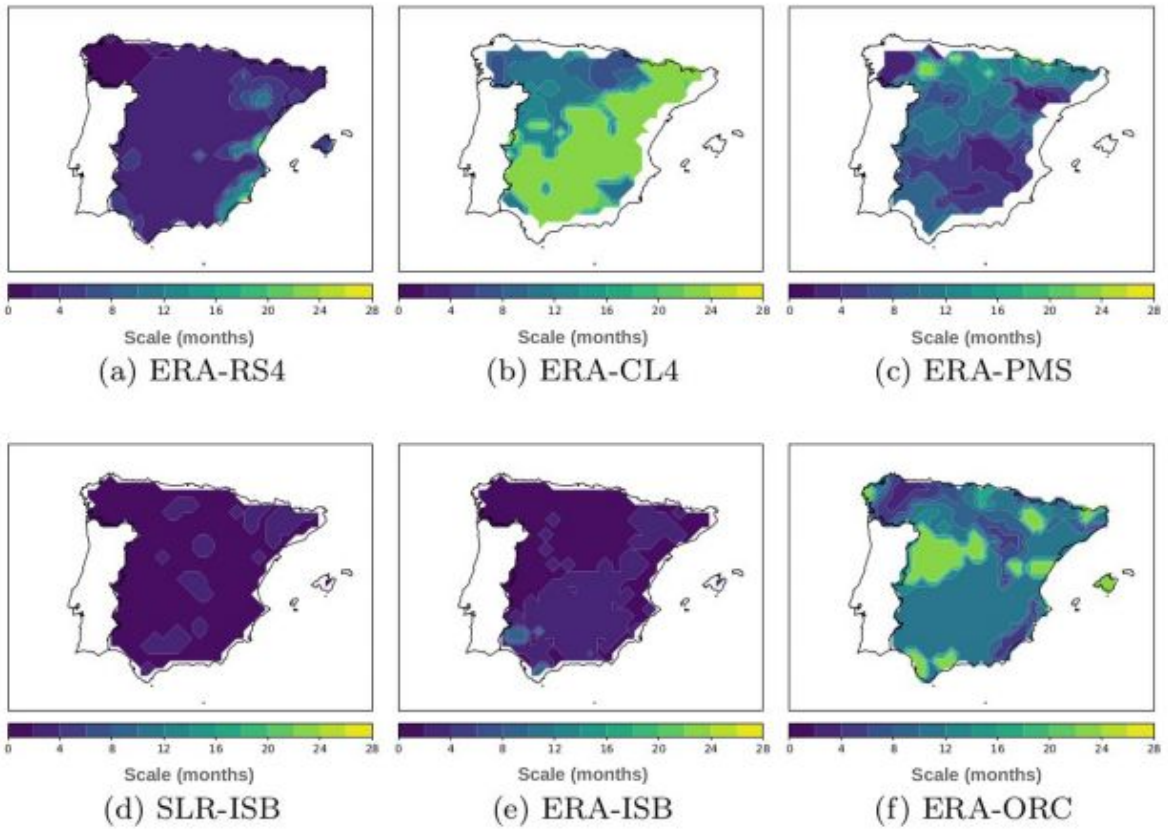

Figure 5.2.2.2 The nx timescale maximizing the correlation between the SPI-nx and SSMI-1 for the RCM and LSM simulations. Portugal and regions from the study area (mainland Spain) whose values are not within the colour scale are represented in white.

For the RCMs we apply the same procedure. nx maps from Fig. 5.2.2.2 indicates the scale in months at which the correlation between the SSMI-1 and SPI-n is maximal and thus the temporal scale at which meteorological drought propagates to soil moisture drought. Figure 5.2.2.2.a–c shows RCM maps, whereas Fig. 5.2.2.2.d–f shows ISB and ORC LSM (reference data) maps. The scale ranges from 0 to 28 months, with the dynamics of the model in regions with a yellowish tone being slower than those in regions with a bluish tone.

Panels a-c show that the RCMs provide different results even though they use the same driving data, which indicates the predominance of model structure with respect to the driving data. This becomes more evident when a RCM is compared to the LSM that has the same surface scheme. For example, the RS4 and ISB (Panels a, d, and e) maps show similar spatial patterns. These are very homogeneous, with scales that range from 1 to 4 months, implying that ISB reacts very quickly to precipitation. Another example is the comparison between PMS and ORC (Panels c and f). Both models show greater heterogeneity than ISB, with scales from 1 to 20 (PMS) and 24 (ORC) months, highlighting the role of the continental surface. Finally, the CL4 (Panel b) behaviour is quite homogeneous. The peninsula is divided into two areas, one over the northwest, where the nx scale ranges between 6 and 12 months, and a larger one with a fixed value of 20 months. It is interesting to note the similar spatial structures from the ERA-CL4 and ERA-ISB maps (Panels b and e), indicating that soil moisture drought propagation by CL4 drags the same spatial structures as its driving data

5.3. Hydrological Drought

5.3.1. Hydrological Drought Indices

Here, we evaluate the ability of the models to simulate streamflow drought (SSI). In this case, we compare the ability directly with that of the SMP-SMP, assuming that it provides a good estimate of natural flows. Figure 5.3.1.1. shows the RMSDs for the different simulations, with lower values indicating higher skills. SFR-DIF generally has the smallest RMSDs, ranging from 0.6 to 0.8, with maximum values between 0.8 and 1.0 in an area at the headwaters of the Tajo, Guadiana, and Júcar, which also includes the southernmost stations in the Ebro river basin. SFR-3L presents similar results, whereas the SFR-LHD exhibits larger RMSDs at most stations, with a maximum value of approximately 1.2. The aforementioned high baseflows in this model are likely the cause of these large RMSDs, which impact its capability to reproduce drought status. To put all of these results in the context of drought studies, an RMSD value of 1 represents one standard deviation of the index and, thus, even errors of 0.6, which is the best case for all simulations and may change the drought status of a given monthly flow (i.e., from normal to drought status). Concerning the effect of forcing, the maps show that the MSW has similar results to the SFR, while E2O, in general, yields somewhat larger RMSDs

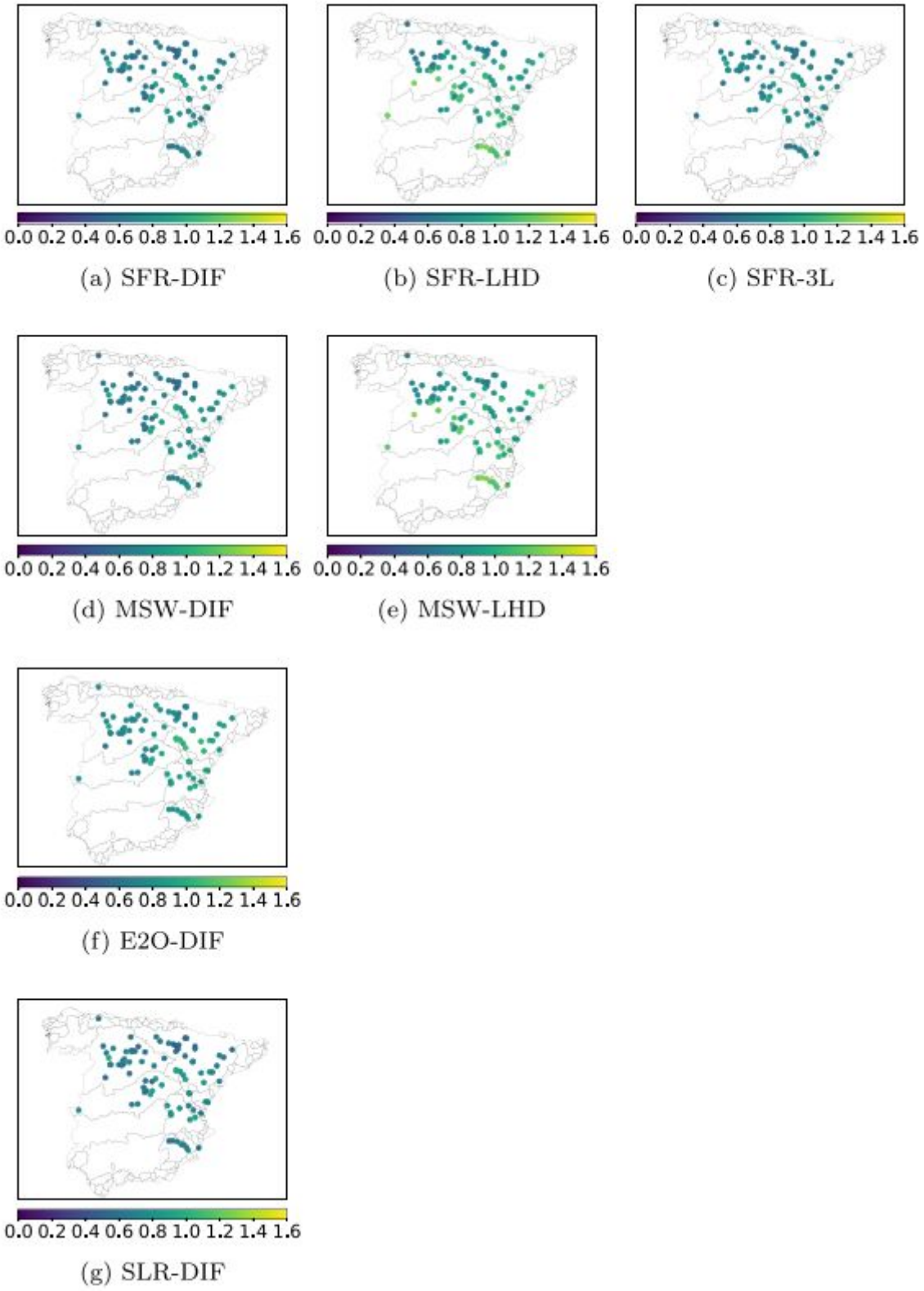

Figure 5.3.1.1. RMSD of the SSI (compared to the SMP-SMP) for the simulations performed in this study

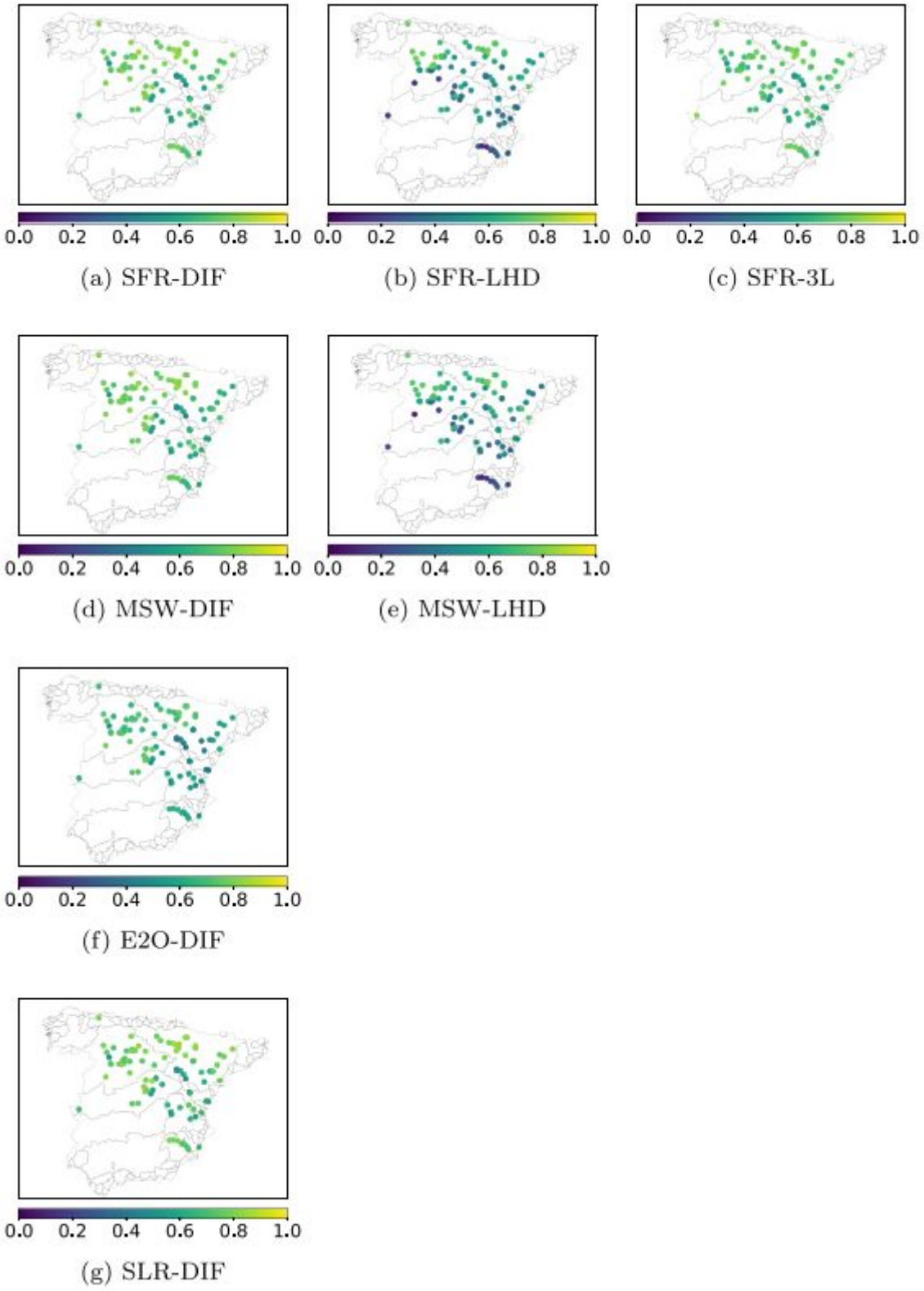

Figure *5.3.1.2.* Pearson correlation (r) of the SSI (compared to the SMP-SMP) for the simulations performed in this study

Figure 5.3.1.2 depicts the Pearson correlation coefficient (r) of the same simulations, with higher values representing better performances. The SFR-DIF is, again, the simulation with the best scores, followed by SFR-3L and SFR-LHD. In the last case, the correlations in some rivers are extremely low, especially in the southern half of the area of study, where summer flows are minimal and, thus, negatively affected by the high baseflow bias in the LHD. The impact of changing the forcing datasets remains low, as it was before

The conclusion of this comparison is that, in terms of the SSI, model formulation is the most important uncertainty source compared to the forcing dataset.

5.3.2. Propagation of drought to runoff and streamflow

Finally, we evaluate how the models simulate drought propagation from precipitation to streamflow. We have studied the correlation between the SPI-n and SSI for different values of n (not shown). We found that, in general, the SMP-SMP has a behavior closer to the DIF and 3L behaviors compared with the observations in many basins. This means that even a well-tested hydrological model, such as the SMP, has difficulties producing the right correlations between the SPI-n and SSI. For its part, the LHD presents a different behavior due to the connection of rivers to the groundwater in this model. In all cases, the simulations are closer to the other simulations when using the same model and not the same forcing dataset, which indicates that model formulation largely determines the drought propagation behavior, and the forcing dataset has a reduced impact.

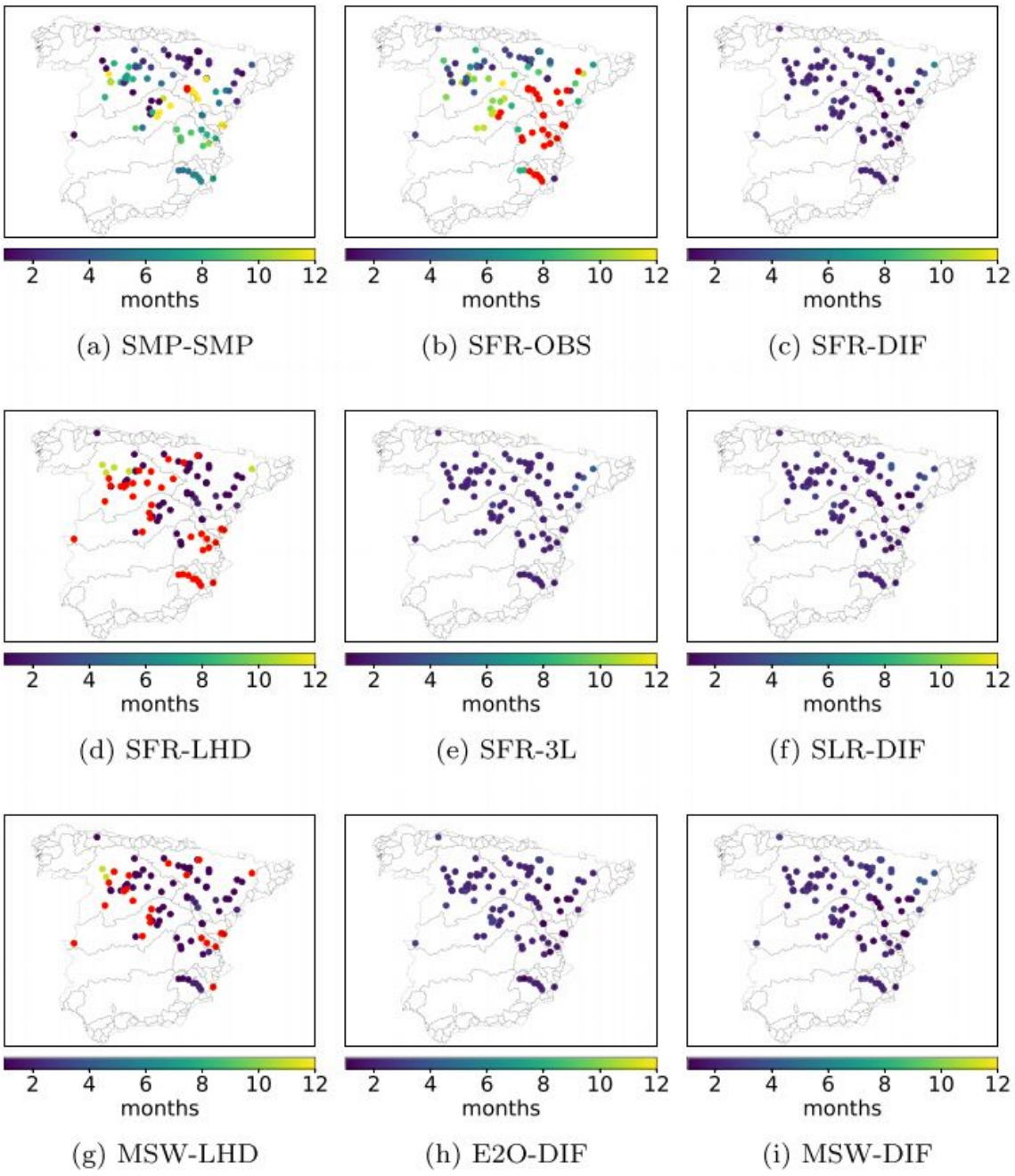

Figure 5.3.2.1. nx scale, in months, of the SPI-n, which better correlates with the SSI. The red dots indicate scales longer than 12 months

We now generalize for the whole study area. Figure *5.3.2.1.* shows the scale nx , in months, of the SPI-n that better correlates with the SSI. The SFR-OBS (b) compares basin precipitation from the SFR and observed SSI at each station. There are many red dots in areas where the flow is highly intervened by water management, but other reasons cannot be excluded, such as karsts or groundwater influence, because some red dots correspond to rivers in the natural regime. The SMP-SMP (a) is the result of a well-tested hydrological model; however, we must keep in mind that it is not the ground truth, and it will not be able to correctly simulate the presence of large karst systems or other complex geological features;

therefore, it does not have a perfect skill score, as discussed previously. The SMP-SMP shows some coherent geographical patterns, with low nx values (1-3 months) in the north in most of the Ebro and in some areas of the Duero and Tajo basins. The highest values (reaching 1 year) are found in the Sistema Iberico mountain range, separating the Ebro and Duero basins. Moderate values occur in the SE and some areas of the Duero basin. With regard to the other models, The DIF and 3L present the lowest nx , as in the case of the root-zone soil moisture, indicating the generally fast response of rivers to precipitation deficits. The comparison with the SMP shows that these nx values are too low and too homogeneous in space. Forcing the DIF with the SLR instead of the SFR, MSW or E2O does not change the results significantly, suggesting that those results are mostly dependent on model formulation. Indeed, a model with a different approach, such as the LHD, presents a divergent behavior, with high values of nx in many of the studied basins, which is likely due to the role of groundwater buffering the streamflow response to drought. Furthermore, it is more sensitive to forcing than the other models, as was the case for soil moisture.

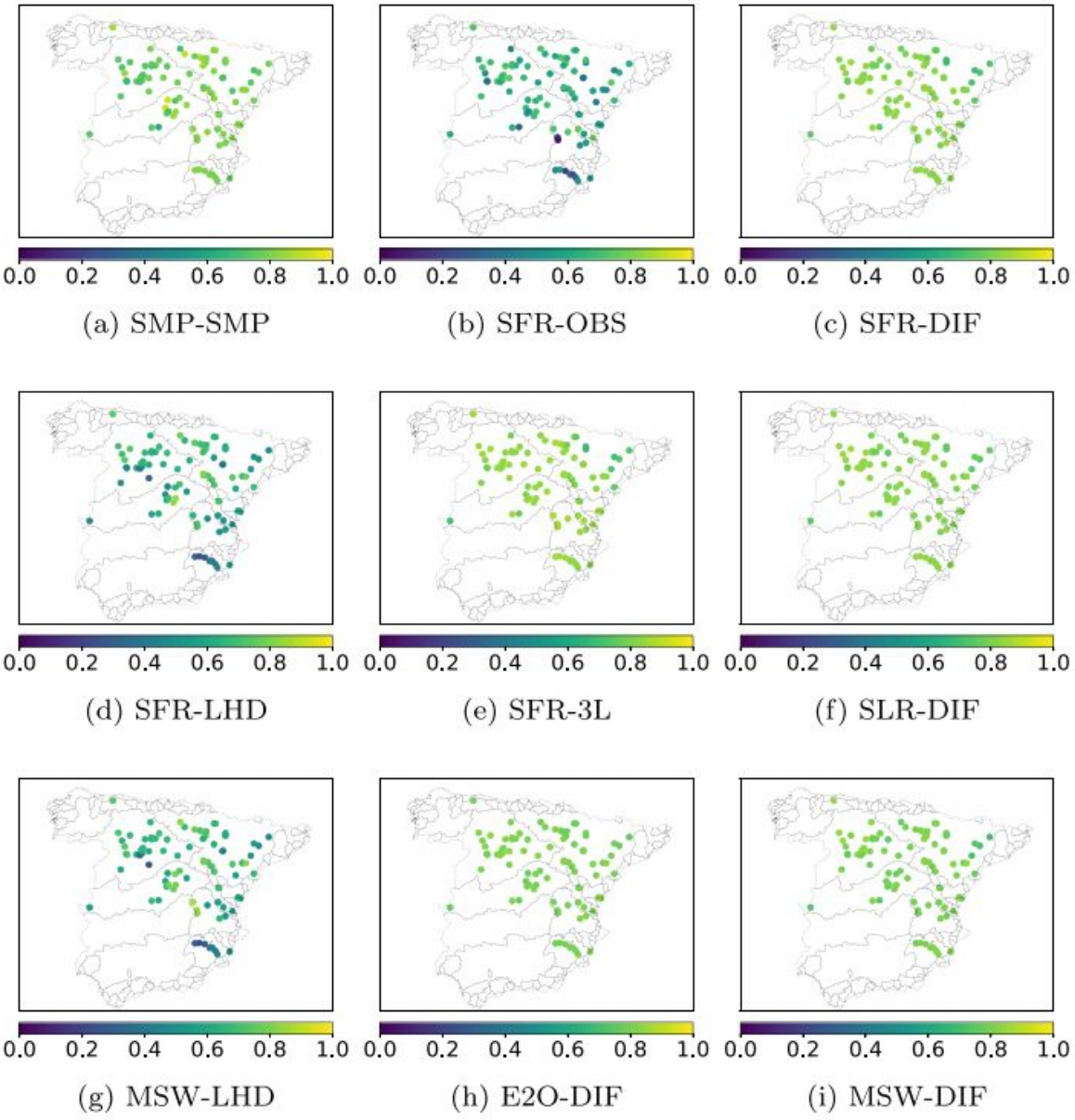

Figure 5.3.2.2. Pearson correlation between the SPI-n and SSI when n is the scale that maximizes the correlation (nx)

Figure 5.3.2.2. shows the Pearson correlation between the SPI-n and SSI when n = nx . If we compare the SFR-OBS with the SMP-SMP, we see that in the real world, which is complex and influenced by water management, the correlations between the SPI-nx and SSI are lower than those in the non-human influenced and simplified world of a model. This result suggests that, in reality, there are many more factors driving streamflow variability, as defined by the SSI, than just precipitation. As expected, the DIF and 3L streamflow variabilities are too related to precipitation (i.e., high correlation), as they do not simulate management or groundwater processes; however, they are quite comparable to the SMP-SMP. The LHD, on the contrary, has much lower correlations, which means that the streamflow variability in this case is driven by other factors, such as groundwater processes.

Basin	Area (km²)	Gauging station's code	RCMs			SIMPA	
			ERA-RS4	ERA-CL4	ERA-PMS	SMP-SMP	SMP-OBS
Duero	41808	2062	3	12	3	9	9
Ebro	40434	9011	2	8	1	2	3
Duero	36570	2054	3	9	3	9	9
Ebro	25194	9002	2	8	1	1	3
Duero	15638	2097	3	**13**	3	8	10
Duero	14283	2043	3	**13**	3	8	10
Ebro	12782	9025	2	1	1	2	8
Ebro	12010	9120	3	6	3	1	3

Table 5.3.2.1. The nx timescale maximizing the correlation between the SPI-nx and (i) SRI-1 (RCMs) and (ii) SSI-1 (SMP and OBS). Scales longer than 12 months are marked in bold. A colour scale has been included to indicate the strength of the correlations between the SPI-nx and (i) SRI-1 and (ii) SSI-1 following the guide proposed by Evans (1996). The correlation ranges and the associated colours are as follows: (i) very strong, 0.80–1.0 (yellow); (ii) strong, 0.60–0.79 (blue); (iii) moderate, 0.40-0.59 (white); and (iv) weak, 0.20–0.39 (red).

Table *Table 5.3.2.1.* shows the nx values that indicate the monthly scale at which the correlation between the SPI-nx and (i) SRI-1 (RCMs) and (ii) SSI-1 (SMP and OBS) is maximal. This can be interpreted as the temporal scale at which meteorological drought propagates to hydrological drought. To better understand these results and the extent to which they reflect the propagation of a precipitation anomaly to a streamflow anomaly, a colour scale is included to indicate the strength of the correlation. It follows the guideline given by Evans (1996): very strong (yellow), strong (blue), moderate (white), and weak (red).

In contrast to what we saw previously RS4 and PMS show very similar scales: means of 3 months for stations in the Duero Basin and 2 months (RS4) and 1 month (PMS) for stations in the Ebro Basin. However, CL4 provides larger scales, from 9 to 13 months (Duero Basin) and from 1 to 8 months (Ebro Basin). The difference in scales shown by the RCMs is an indicator of the relevance of model structure in drought propagation.

The RCMs and SMP show higher nx values and thus slower dynamics in the Duero Basin than in the Ebro Basin. This is in agreement with the nx values obtained using the SSI-1 computed with OBS, in which the mean nx values are 9 (Duero) and 4 (Ebro). Analysing these results, we can establish that the RS4 and PMS runoff responds quickly to precipitation anomalies. When compared to SMP and OBS, the monthly scales provided are

in good agreement in the Ebro Basin but are too low in the Duero Basin. In contrast, CL4 shows larger scales and behaves inversely to RS4 and PMS, as it is in better agreement with SMP and OBS in the Duero Basin.

Focusing on the strength of the correlations, RS4 (coupled to ISB) shows strong positive correlations at six of the eight stations analysed, indicating that precipitation has a significant role in streamflow variability. However, the correlations of CL4 and PMS with the SPI-nx are moderate (even weak for station number 9025), which implies that there are also other factors driving this variability.

6. Discussion

In this study, we have shown that, despite their limitations, global forcing datasets can be useful for drought studies. The MSW, which integrates diverse sources of data, including rain gauges and satellites, is a valuable dataset and represents a clear improvement compared with the E2O in both absolute and relative (drought) terms (see the electronic supplementary material). However, we should not forget that the MSW uses rain gauge data and, thus, is probably better in data rich countries, such as Spain, than in countries where observations are inexistent or unavailable.

RCMs provide a good representation of meteorological drought. The results show that they are capable of reproducing the same drought spells as those detected by their driving data and the reference data. However, they differ in terms of an event's duration, severity, and area, as expected. We have identified that RCMs improve drought representation with respect to the driving data in several aspects. For instance, the temporal evolution of the SPI-12 shows that the severity of some of the drought spells is closer to that of the reference data. In addition, they do not reproduce the spurious trend identified in the driving data, which could lead to a misrepresentation of the phenomenon. Finally, a temporal correlation analysis shows that drought representation is improved over the northeastern region of the Iberian Peninsula, which is a known limitation of global analysis across Spain. These results are consistent with previous studies showing that RCMs provide a suitable representation of drought using drought indices across Spain (Barrera-Escoda et al., 2013; Maule et al., 2013; García-Valdecasas Ojeda et al., 2017).

However, our study shows that our implementation of state-of-the-art LSMs in Spain is not yet ready to provide reliable information to water managers. We compared the differences among the SSMI used in several simulations, concluding that changing the forcing dataset and keeping the same model has a larger impact on the results than the opposite, which implies that the forcing dataset plays an important role. These comparisons mixed both the spatial and temporal components of the error, but it is the spatial component that amplifies the divergences among the simulations, as there are large differences between how, for instance, E2O and SFR represent the spatial structures of drought.

The results also show that model formulations have a strong influence on the temporal scale nx at which the precipitation variability (SPI) affects the soil moisture variability (SSMI). This is an important issue because it implies that since there is no ground truth for comparison, we cannot trust land-surface models to understand how drought propagates to soil moisture. The spatial structures of nx are overly homogeneous in space in the 3L and DIF. Even though we do not know what the reality is, intuition tells us that there should be differences across various hydrological settings and climates. LHD, on the contrary, presents a rich spatial variability of nx , which shows the important effects that groundwater lateral flows and the water table have on soil moisture dynamics. This is especially important in semiarid areas, where the interaction between the water table and soil moisture sustains vegetation during the dry season and drought periods. Furthermore, the differences among models can be amplified by the choice of the forcing dataset, as the results for the LHD have shown that changing the forcing dataset alters how precipitation variability propagates to soil moisture. As a consequence, model formulation is the key factor explaining the uncertainty of drought propagation to soil moisture, while forcing explains most of the divergence when representing the spatial structures of drought, as global products are not able to reproduce the finer scale spatial details of the precipitation pattern.

Concerning RCMs, the results regarding soil moisture and hydrological drought representation show differences when RCMs are compared among themselves and to the reference data. The analyses are carried out using the RMSD and Pearson correlations, and the observed uncertainty corresponds, in most cases, to a change in the drought category (according to the SPI drought classification) of RCMs with respect to the reference data. . LSM offline simulations are used as reference datasets for soil moisture drought analysis due to the lack of observations, which is not ideal. There is not enough in-situ data available for such a study. Remote sensing products could also be an option, but there are certain limitations that should be taken into account, for example, uncertainty sources, gaps in the data, and short time series (AghaKouchak et al., 2015). Escorihuela and Quintana-Seguí (2016) showed that different satellite products behave differently across a region representative of Mediterranean landscapes (Catalonia in the northeast Iberian Peninsula). Therefore, using these products would add more uncertainty to the study. In addition, the retrieved soil moisture data correspond to surface soil moisture, and, in this study, we considered root zone soil moisture.

The structural differences among models affect their ability to simulate the SSI; thus, model formulation is the most important uncertainty source in the SSI results. One of the interesting results in drought propagation is that, compared with the observations at the near natural flow stations, the correlation between the SPI-nx and SSI is generally too high for the SMP, DIF and 3L. This means that these models miss important processes affecting the SSI. As the model structure is the most important source of uncertainty, it is meaningful to use global forcing datasets for local (national or large basin scale) streamflow drought studies. Concerning RCMs, a key result of the study is the relevance of the models' physics, which prevails over the driving data. This is shown in the soil moisture and hydrological drought representation evaluation as well as in the analyses of drought propagation. In the latter case, the model's structure influences the temporal scale at which the variability in precipitation affects that of soil moisture and streamflow.

One of the main results of this study is that the land-surface models used in this study must be improved if they are going to be used to monitor and understand drought processes in Spain. This is mainly due to the large uncertainty in the simulation of soil-moisture and the needed improvement in groundwater processes and their interactions with soil and rivers. We believe that similar results would be obtained if more models were introduced in the comparison, as the main causes of the detected problems are shared by many LSMs. However, this should be the subject of a larger future study. Therefore, future work in improving offline LSMs is necessary not only to provide interesting data for water management (planning and monitoring) but to prepare for the next generation of earth-system models. In this respect, the methodology used in this study, which compares different kinds of drought and its propagation, is useful to reveal structural differences and problems in model simulations, providing new perspectives that go beyond the validation of the absolute values of the studied variables.

7. Conclusions and perspectives

Land-surface models are tools that have the potential to provide valuable information to water managers. Simulated standardized soil moisture is especially interesting as a drought index because soil moisture integrates the effects of effective precipitation and actual evapotranspiration. LSMs can provide estimations of this index, compensating for the lack of observations. Also, in the context of climate change, we need to know the future evolution of drought. To this aim, we may use RCMs, but we need to know how these behave in terms of drought, which is what we have evaluated in this study.

However, this study shows that the uncertainties due to model formulation remain an important issue in current generation large-scale hydrological simulations based on landsurface models. This is true for the results of both the standardized soil moisture (SSMI) and streamflow (SSI), for offline LSMs and for RCMs.

In the case of soil moisture, the differences among LSM simulations are quite large both in terms of the RMSD and correlation. Furthermore, the differences in how drought propagates to soil moisture are also large and determined by the model structure. The problem is difficult to solve because there is no Spanish dataset with in situ root-zone soil moisture data that could be used to guide model improvement and, thus, models cannot be effectively constrained and validated, even though some good networks exist: REMEDHUS (https://ismn.geo.tuwien.ac.at/networks/remedhus/) and the Valencia Anchor Station (Coll Pajaron´ 2017).

For streamflow, the quality of the simulated SSI by LSMs is not as good, as it would otherwise be desirable. Furthermore, the LSMs are not able to correctly simulate the scales of drought propagation, and they miss processes that affect the SSI, as the correlations between precipitation (SPI-nx) and streamflow (SSI) are too high (this is also true for the SMP).

The forcing datasets do have an impact on the uncertainty of the results but, in general, this impact is not as large as the impact of uncertainty due to model formulation. The MSW, which includes satellite precipitation data, represents a large improvement compared with E2O.

It is concluded that RCMs provide added value to meteorological drought representation, minimizing possible error sources from the driving data and ameliorating its characterization over areas that are known to pose certain problems to global driving data products. However, soil moisture and hydrological drought representation by RCMs show uncertainties. This is mainly due to the relevance of model physics and its prevalence to the driving data. Similar results were obtained for the propagation processes, in which model structure was found to influence the dynamics of drought propagation, showing different temporal scales depending on how precipitation variability is formulated within the model.

LSMs and RCMs are a suitable tool for meteorological drought studies but should be used cautiously for soil moisture and hydrological drought analyses. Improvements regarding soil moisture modelling and streamflow-related processes (natural and anthropic) should be performed to better characterize drought events as well as their propagation

The methodologies used to study drought propagation are not only useful to understand this process but also to explore structural problems in models and guide model improvement. In the future, it is necessary to continue improving the current hydrological implementation of LSMs in Spain (SASER and LEAFHYDRO). The assimilation of the remote sensing of surface soil moisture can be a useful way to improve how models simulate root-zone soil moisture. Concerning streamflow, the main physical processes to be improved are those related to groundwater and lateral flows, which need to be introduced in SASER (3L and DIF) and improved in LEAFHYDRO. Finally, it would also be necessary to introduce human-related processes in models, such as irrigation and dam operation, in order to be able to compare them to reality and study the direct impacts of humans on drought.

In future studies, in the context of HUMID project, we will explore aspects related to human processes, which we did not cover in this report. Also, being drought a multivariate physical process, we will study the role of evapotranspiration in drought, and its interaction with other variables, such as precipitation and soil moisture, during drought events.

References

AghaKouchak A, Farahmand A, Melton FS, Teixeira J, Anderson MC, Wardlow BD, Hain CR (2015) Remote sensing of drought: progress, challenges and opportunities. Rev Geophys 53(2):452–480. https://doi.org/10.1002/2014RG000456

Anagnostopoulou, C.: Drought episodes over Greece as simulated by dynamical and statistical downscaling approaches, Theor. Appl. Climatol., 129, 587–605. https://doi.org/10.1007/s00704-016-1799-5, 2017

Andreadis, K. and Lettenmaier, D.: Trends in 20th century drought over the continental United States, Geophys. Res. Lett., 33, L10403. https://doi.org/10.1029/2006GL025711, 2006

Balsamo G, Albergel C, Beljaars A, Boussetta S, Brun E, Cloke H, Dee D, Dutra E, Pappenberger F, de Rosnay P, Muñoz-Sabater J, Stockdale F, Vitart F (2012) ERA-Interim/land: A global land-surface reanalysis based on ERA-interim meteorological forcing. Technical report, ECMWF

Barker LJ, Hannaford J, Chiverton A, Svensson C (2015) From meteorological to hydrological drought using standardised indicators. Hydrol Earth Syst Sci Discuss 12(12):12,827–12,875. https://doi.org/10.5194/hessd-12-12827-2015

Barrera-Escoda, A., Goncalves, M., Guerreiro, D., Cunillera, J., and Baldasano, J.: Projections of temperature and precipitation extremes in the North Western Mediterranean Basin by dynamical downscaling of climate scenarios at high resolution (1971–2050), Climatic Change, 122, 567–582. https://doi.org/10.1007/s10584-013-1027-6, 2013

Beck HE, van Dijk AIJM, Levizzani V, Schellekens J, Miralles DG, Martens B, de Roo A (2017) MSWEP: 3-hourly 0.25 global gridded precipitation (1979-2015) by merging gauge, satellite, and reanalysis data. Hydrol Earth Syst Sci 21(1):589–615. https://doi.org/10.5194/hess-21-589-2017.

Beguería S, Vicente-Serrano SM, Reig F, Latorre B (2014) Standardized precipitation evapotranspiration index (SPEI) revisited: Parameter fitting, evapotranspiration models, tools, datasets and drought monitoring. Int J Climatol 34 (10):3001–3023. https://doi.org/10.1002/joc.3887

Belo-Pereira, M., Dutra, E., and Viterbo, P.: Evaluation of global precipitation data sets over the Iberian Peninsula, J. Geophys. Res., 116, D20101. https://doi.org/10.1029/2010JD015481, 2011, b.

Beuvier, J., Sevault, F., Herrmann, M., Kontoyiannis, H., Ludwig, W., Rixen, M., Stanev, E., Béranger, K., and Somot, S.: Modeling the Mediterranean Sea interannual variability during 1961–2000: Focus on the Eastern Mediterranean Transient, J. Geophys. Res., 115, C08017. https://doi.org/10.1029/2009JC005950, 2010.

Bindlish R, Jackson T, Cosh M, Zhao T, O'Neill P (2015) Global Soil Moisture From the Aquarius/SAC-D Satellite: Description and Initial Assessment. IEEE Geosci Remote Sens Lett 12(5):923–927. https://doi.org/10.1109/LGRS.2014.2364151.

Blenkinshop, S. and Fowler, H.: Changes in drought frequency, severity and duration for the British Isles projected by the PRUDENCE regional climate models, J. Hydrol., 342, 50–71, 2007a.

Boone A (2000) Modélisation des processus hydrologiques dans le schéma de surface ISBA: Inclusion d'un réservoir hydrologique, du gel et modélisation de la neige. PhD thesis, Université Paul Sabatier (Toulouse III), http://www.cnrm.meteo.fr/IMG/pdf/boone_thesis_2000.pdf

Boone A, Calvet JC, Noilhan J (1999) Inclusion of a Third Soil Layer in a Land Surface Scheme Using the Force–Restore Method. J Appl Meteorol 38(11):1611–1630. https://doi.org/10.1175/1520-0450(1999)038%3C1611:IOATSL%3E2.0.CO;2

Bowden, J., Talgo, K., Spero, T., and Nolte, C.: Assessing the Added Value of Dynamical Downscaling Using the Standardized Precipitation Index, Adv. Meteorol., 2016, 8432064. https://doi.org/10.1155/2016/8432064, 2016

Castro, M., Fernández, C., and Gaertner, M. A.: Description of a Mesoscale Atmospheric Numerical Model, in: Mathematics, Climate and Environment, edited by: Diaz, J. I. and Lions, J. L., Rech. Math. Appl. Ser. Mason, 55, 230–253, 1993, b.

Christensen, J., Carter, T., Rummukainen, M., and Amanatidis, G.: Evaluating the performance and utility of regional climate models: the PRUDENCE approach, Climatic Change, 81, 1–6, 2007.

Colin, J., Déqué, M., Radu, R., and Somot, S.: Sensitivity study of heavy precipitations in Limited Area Model climate simulations: influence of the size of the domain and the use of the spectral nudging technique, Tellus A, 62, 591–604, https://doi.org/10.1111/j.1600-0870.2010.00467.x, 2010.

Coll Pajarón MA (2017) Distribución de la humedad del suelo mediante observaciones del satélite SMOS, modelización con SURFEX y medidas in situ sobre la Valencia Anchor Station. Phd, Universitat de València, http://roderic.uv.es/handle/10550/60877.

David CH, Habets F, Maidment DR, Yang ZLL (2011a) RAPID applied to the SIM-France model, vol 25. https://doi.org/10.1002/hyp.8070. https://hal.archives-ouvertes.fr/hal-00641722/document

de Luis, M., Brunetti, M., González-Hidalgo, J. C., Longares, L. A., and Martín-Vide, J.: Changes in seasonal precipitation in the Iberian Peninsula during 1946–2005, Global Planet. Change, 74, 27–33. https://doi.org/10.1016/j.gloplacha.2010.06.006, 2010

de Rosnay, P. and Polcher, J.: Modelling root water uptake in a complex land surface scheme coupled to a GCM, Hydrol. Earth Syst. Sci., 2, 239–255. https://doi.org/10.5194/hess-2-239-1998, 1998, b

Decharme, B., Alkama, R., Douville, H., Becker, M., and Cazenave, A.: Global Evaluation of the ISBA-TRIP Continental Hydrological System. Part II: Uncertainties in River Routing Simulation Related to Flow Velocity and Groundwater Storage, J. Hydrometeor., 11, 601–617. https://doi.org/10.1175/2010JHM1212.1, 2010

Dee DP, Uppala SM, Simmons a J, Berrisford P, Poli P, Kobayashi S, Andrae U, Ma Balmaseda, Balsamo G, Bauer P, Bechtold P, Beljaars a C M, van de Berg L, Bidlot J, Bormann N, Delsol C, Dragani R, Fuentes M, Geer a J, Haimberger L, Healy SB, Hersbach H, Hólm E V, Isaksen L, Kållberg P, Köhler M, Matricardi M, McNally aP, Monge-Sanz BM, Morcrette JJ, Park BK, Peubey C, de Rosnay P, Tavolato C, Thépaut JN, Vitart F (2011) The ERA-interim reanalysis:

configuration and performance of the data assimilation system. Q J R Meteorol Soc 137(656):553–597. https://doi.org/10.1002/qj.828

del Río, S., Herrero, L., Pinto-Gomes, C., and Penas, A.: Spatial analysis of mean temperature trends in Spain over the period 1961–2006, Global Planet. Change, 78, 65–75. https://doi.org/10.1016/j.gloplacha.2011.05.012, 2011

Déqué, M. and Somot, S.: Analysis of heavy precipitation for France using ALADIN RCM simulations, Idöjaras Q. J. Hungarian Meteorological Service, 112, 179–190, 2008

Domínguez, M., Gaertner, M. A., de Rosnay, P., and Losada, T.: A regional climate model simulation over West Africa: Parameterization tests and analysis of land-surface fields, Clim. Dynam., 35, 249–265, 2010, b.

Domínguez, M., Romera, R., Sánchez, E., Fita, L., Fernández, J., Jiménez-Guerrero, P., Montávez, J., Cabos, W., Liguori, G., and Gaertner, M.: Present-climate precipitation and temperature extremes over Spain from a set of high resolution RCMs, Clim. Res., 58, 149–164. https://doi.org/10.3354/cr01186, 2013.

Durand Y, Brun E, Merindol L, Guyomarc'h G, Lesaffre B, Martin E (1993) A meteorological estimation of relevant parameters for snow models. Ann Glaciol 18:65–71.

Durand Y, Giraud G, Brun E, Merindol L, Martin E (1999) A computer-based system simulating snowpack structures as a tool for regional avalanche forecasting. J Glaciol 45(151):469–484

ECMWF: ERA-Interim, available at: https://www.ecmwf.int/en/forecasts/datasets/archive-datasets/reanalysis-datasets/era-interim, last access: 29 October 2019.

Edossa, D., Babel, M., and Das Gupta, A.: Drought Analysis in the Awash River Basin, Ethiopia, Water Resour. Manag., 24, 1441–1460. https://doi.org/10.1007/s11269-009-9508-0, 2009.

Entekhabi D, Njoku EG, O'Neill PE, Kellogg KH, Crow WT, Edelstein WN, Entin JK, Goodman SD, Jackson TJ, Johnson J, Kimball J, Piepmeier JR, Koster RD, Martin N, McDonald KC, Moghaddam M, Moran S, Reichle R, Shi JC, Spencer MW, Thurman SW, Tsang L, Van Zyl J (2010) The Soil Moisture Active Passive (SMAP) Mission. Proc IEEE 98(5):704–716. https://doi.org/10.1109/JPROC.2010.2043918, http://ieeexplore.ieee.org/document/5460980/

Escorihuela MJ, Merlin O, Escorihuela A, Quintana P, Martinez D (2012) SMOSCAT: Towards operational high resolution Soil Moisture with SMOS. In: 2012 IEEE International Geoscience and Remote Sensing Symposium. IEEE, pp 3784–3786. https://doi.org/10.1109/IGARSS.2012.6350493, http://ieeexplore.ieee.org/document/6350493/

Escorihuela MJ, Quintana-Seguí P (2016) Comparison of remote sensing and simulated soil moisture datasets in Mediterranean landscapes. Remote Sens Environ 180:99–114. https://doi.org/10.1016/j.rse.2016.02.046.

Escorihuela, M. J. and Quintana-Seguí, P.: Comparison of remote sensing and simulated soil moisture datasets in Mediterranean landscapes, Remote Sens. Environ., 180, 99–114. https://doi.org/10.1016/j.rse.2016.02.046, 2016.

Estrela T, Quintas L (1996) El sistema integrado de modelización precipitación-aportación SIMPA. Rev Ing Civ 104:43–52.

Evans, J.: Straightforward Statistics for the Behavioral Sciences, Pacific Grove, CA, Brooks/Cole Publishing, 1996, b, c, d.

Fan Y, van den Dool HM, Wu W (2011) Verification and intercomparison of multimodel simulated land surface hydrological datasets over the united states. J Hydrometeorol 12(4):531–555. https://doi.org/10.1175/2011JHM1317.1

FAO: The State of Food Insecurity in the World, Rome, Italy, FAO, 2009

Farahmand A, AghaKouchak A (2015) A generalized framework for deriving nonparametric standardized drought indicators. Adv Water Resour 76:140–145. https://doi.org/10.1016/j.advwatres.2014.11.012.

Farda, A., Déqué, M., Somot, S., Horányi, A., Spiridonov, V., and Tóth, H.: Model ALADIN as regional climate model for Central and Eastern Europe, Stud. Geophys. Geod., 54, 313–332. https://doi.org/10.1007/s11200-010-0017-7, 2010.

Faroux, S., Kaptué Tchuenté, A. T., Roujean, J.-L., Masson, V., Martin, E., and Le Moigne, P.: ECOCLIMAP-II/Europe: a twofold database of ecosystems and surface parameters at 1 km resolution based on satellite information for use in land surface, meteorological and climate models, Geosci. Model Dev., 6, 563–582. https://doi.org/10.5194/gmd-6-563-2013, 2013

Feser, F., Rockel, B., von Storch, H., Winterfeldt, J., and Zahn, M.: Regional Climate Models Add Value to Global Model Data: A Review and Selected Examples, B. Am. Meteorol. Soc., 92, 1181–1192. https://doi.org/10.1175/2011BAMS3061.1, 2011

Gandin LS (1966) Objective analysis of meteorological fields. By L. S. Gandin. Translated from the Russian. Jerusalem (Israel Program for Scientific Translations). Q J R Meteorol Soc 92(393):447–447. https://doi.org/10.1002/qj.49709239320

García-Valdecasas Ojeda, M., Gámiz-Fortis, S. R., Castro-Díez, Y., and Esteban-Parra, M.: Evaluation of WRF capability to detect dry and wet periods in Spain using drought indices, J. Geophys. Res.-Atmos., 122, 1569–1594. https://doi.org/10.1002/2016JD025683, 2017, b, c

Giorgi, F., Jones, C., and Asrar, G.: Addressing climate information needs at the regional level: The CORDEX framework, WMO Bull, 58, 175–183, 2009.

Gupta, H. V., Kling, H., Yilmaz, K. K., and Martínez, G. F.: Decomposition of the mean squared error and NSE performance criteria: Implications for improving hydrological modelling, J. Hydrol., 377, 80–91, https://doi.org/10.1016/j.jhydrol.2009.08.003, 2009.

Habets F, Boone A, Noilhan J (2003) Simulation of a Scandinavian basin using the diffusion transfer version of ISBA. Glob Planet Chang 38(1-2):137–149.

Herrmann, M., Somot, S., Calmanti, S., Dubois, C., and Sevault, F.: Representation of spatial and temporal variability of daily wind speed and of intense wind events over the Mediterranean Sea using dynamical downscaling: impact of the regional climate model configuration, Nat. Hazards Earth Syst. Sci., 11, 1983–2001, https://doi.org/10.5194/nhess-11-1983-2011, 2011.

Hoerling, M., Eischeid, J., Perlwitz, J., Quan, X., Zhang, T., and Pegion, P.: On the Increased Frequency of Mediterranean Drought, J. Climate, 25, 2146–2161, https://doi.org/10.1175/JCLI-D-11-00296.1, 2012.

IPCC: Climate Change 2007: Impacts, Adaptation and Vulnerability, in: Contribution of Working Group II to the Fourth Assessment Report of the Intergovernmental Panel on Climate Change, edited by: Parry, M. L., Canziani, O. F., Palutikof, J. P., van der Linden, P. J., and Hanson, C. E., Cambridge University Press, Cambridge, UK, 976 pp., 2007.

IPCC: Climate change 2014: Synthesis Report, in: Contribution of Working Groups I, II and III to the Fifth Assessment Report of the Intergovernmental Panel on Climate Change, edited by: Core Writing Team, Pachauri, R. K., and Meyer, L. A., IPCC, Geneva, Switzerland, 151 pp., 2014.

Jacobsen, I. and Heise, E.: A new economic method for the computation of the surface temperature in numerical models, Beitr. Phys. Atm., 55, 128–141, 1982.

Jenkins, K. and Warren, R.: Quantifying the impact of climate change on drought regimes using the Standardised Precipitation Index, Theor. Appl. Climatol., 120, 41–54, https://doi.org/10.1007/s00704-014-1143-x, 2014.

Jiménez-Guerrero, P., Montávez, J. P., Domínguez, M., Romera, R., Fita, L., Fernández, J., Cabos, W. D., Liguori, G., and Gaertner, M. A.: Description of mean fields and interannual variability in an ensemble of RCM evaluation simulations over Spain: results from the ESCENA project, Clim. Res., 57, 201–220, https://doi.org/10.3354/cr01165, 2013.

Kaptue Tchuente, A. T., Roujean, J. L., and Faroux, S.: ECOCLIMAP-II: An ecosystem classification and land surface parameters database of Western Africa at 1 km resolution for the African Monsoon Multidisciplinary Analysis (AMMA) project, Remote Sens. Environ., 114, 961–976, https://doi.org/10.1016/j.rse.2009.12.008, 2010.

Kenawy, A., López-Moreno, J. I., and Vicente-Serrano, S. M.: Summer temperature extremes in northeastern Spain: Spatial regionalization and links to atmospheric circulation (1960–2006), Theor. Appl. Climatol., 113, 387–405, https://doi.org/10.1007/s00704-012-0797-5, 2013.

Kerr YH, Waldteufel P, Richaume P, Wigneron JP, Ferrazzoli P, Mahmoodi A, Al Bitar A, Cabot F, Gruhier C, Juglea SE, Leroux D, Mialon A, Delwart S (2012) The SMOS Soil Moisture Retrieval Algorithm. IEEE Trans Geosci Remot Sens 50(5):1384–1403. https://doi.org/10.1109/TGRS.2012.2184548, http://ieeexplore.ieee.org/document/6161633/

Koster RD, Guo Z, Yang R, Pa D, Mitchell K, Puma MJ (2009) On the nature of soil moisture in land surface models. J Clim 22(16):4322–4335. https://doi.org/10.1175/2009JCLI2832.1

Krinner, G., Viovy, N., de Noblet-Ducoudré, N., Ogée, J., Polcher, J., Friedlingstein, P., Ciais, P., Sitch, S., and Prentice, I.: A dynamic global vegetation model for studies of the coupled atmosphere-biosphere system, Global Biogeochem. Cy., 19, GB1015. https://doi.org/10.1029/2003GB002199, 2005, b

Li, Z. X.: Ensemble Atmospheric GCM Simulation of Climate Interannual Variability from 1979 to 1994, J. Climate, 12, 986–1001, 1999.

Linés C, Werner M, Bastiaanssen W (2017) The predictability of reported drought events and impacts in the Ebro Basin using six different remote sensing data sets. Hydrol Earth Syst Sci 21(9):4747–4765. https://doi.org/10.5194/hess-21-4747-2017

López López P, Wanders N, Schellekens J, Renzullo LJ, Sutanudjaja EH, Bierkens MFP (2016) Improved large-scale hydrological modelling through the assimilation of streamflow and downscaled satellite soil moisture observations. Hydrol Earth Syst Sci 20(7):3059–3076. https://doi.org/10.5194/hess-20-3059-2016.

López-Bustins, J. A., Pascual, D., Pla, E., and Retana, J.: Future variability of droughts in three Mediterranean catchments, Nat. Hazards, 69, 1405–1421. https://doi.org/10.1007/s11069-013-0754-3, 2013

Ma M, Ren L, Yuan F, Jiang S, Liu Y, Kong H, Gong L (2014) A new standardized Palmer drought index for hydro-meteorological use. Hydrol Process 28(23):5645–5661. https://doi.org/10.1002/hyp.10063

Mariotti, A.: Recent Changes in the Mediterranean Water Cycle: A Pathway toward Long-Term Regional Hydroclimatic Change?, J. Climate, 23, 1513–1525. https://doi.org/10.1175/2009JCLI3251.1, 2010

Martínez-Fernández, J., Sánchez, N., and Herrero-Jiménez, C. M.: Recent trends in rivers with near-natural flow regime: The case of the river headwaters in Spain, Prog. Phys. Geog., 37, 685–700, https://doi.org/10.1177/0309133313496834, 2013

Marx A, Kumar R, Thober S, Rakovec O, Wanders N, Zink M, Wood EF, Pan M, Sheffield J, Samaniego L (2018) Climate change alters low flows in Europe under global warming of 1.5, 2, and 3 C. Hydrol Earth Syst Sci 22(2):1017–1032. https://doi.org/10.5194/hess-22-1017-2018.

Masson V, Le Moigne P, Martin E, Faroux S, Alias A, Alkama R, Belamari S, Barbu A, Boone A, Bouyssel F, Brousseau P, Brun E, Calvet JC, Carrer D, Decharme B, Delire C, Donier S, Essaouini K, Gibelin AL, Giordani H, Habets F, Jidane M, Kerdraon G, Kourzeneva E, Lafaysse M, Lafont S, Lebeaupin Brossier C, Lemonsu A, Mahfouf JF, Marguinaud P, Mokhtari M, Morin S, Pigeon G, Salgado R, Seity Y, Taillefer F, Tanguy G, Tulet P, Vincendon B, Vionnet V, Voldoire A (2013) The SURFEXv7.2 land and ocean surface platform for coupled or offline simulation of earth surface variables and fluxes. Geosci Model Dev 6(4):929–960. https://doi.org/10.5194/gmd-6-929-2013

Masson, V., Champeaux, J. L., Chauvin, F., Meriguet, C., and Lacaze, R.: A Global Database of Land Surface Parameters at 1-km Resolution in Meteorological and Climate Models, J. Climate, 16, 1261–1282. https://doi.org/10.1175/1520-0442-16.9.1261, 2003

Masud, M. B., Khaliq, M. N., and Wheater, H. S.: Future changes to drought characteristics over the Canadian Prairie Provinces based on NARCCAP multi-RCM ensemble, Clim. Dynam., 48, 2685–2705. https://doi.org/10.1007/s00382-016-3232-2, 2017

Maule, C. F., Thejll, P., Christensen, J. H., Svendsen, S. H., and Hannaford, J.: Improved confidence in regional climate model simulations of precipitation evaluated using drought statistics from the ENSEMBLES models, Clim. Dynam., 40, 155–173. https://doi.org/10.1007/s00382-012-1355-7, 2013, b

McKee TB, Doesken NJ, Kleist J (1993) Others the relationship of drought frequency and duration to time scales. In: Proceedings of the 8th Conference on Applied Climatology, American Meteorological Society, Boston, MA, Vol 17, pp 179–183.

Meresa, H., Osuch, M., and Romanowicz, R.: Hydro-Meteorological Drought Projections into the 21-st Century for Selected Polish Catchments, Water, 8, 206. https://doi.org/10.3390/w8050206, 2016, b

Merlin O, Escorihuela MJ, Mayoral MA, Hagolle O, Al Bitar A, Kerr Y (2013) Self-calibrated evaporation-based disaggregation of SMOS soil moisture: An evaluation study at 3km and 100m resolution in Catalunya, Spain. Remote Sens Environ 130:25–38. https://doi.org/10.1016/j.rse.2012.11.008.

Miguez-Macho G, Fan Y, Weaver CP, Walko R, Robock A (2007) Incorporating water table dynamics in climate modeling: 2. Formulation, validation, and soil moisture simulation. J Geophys Res Atmos 112(D13):n/a–n/a. https://doi.org/10.1029/2006JD008112

Mishra, A. and Singh, V. P.: Drought modeling – A review, J. Hydrol., 403, 157–175. https://doi.org/10.1016/j.jhydrol.2011.03.049, 2011

MMA (2000) Libro blanco del agua en España. Ministerio de Medio Ambiente

Mo KC, Lettenmaier DP (2014) Objective drought classification using multiple land surface models. J Hydrometeorol 15(3):990–1010. https://doi.org/10.1175/JHM-D-13-071.1

Molero B, Merlin O, Malbéteau Y, Al Bitar A, Cabot F, Stefan V, Kerr Y, Bacon S, Cosh M, Bindlish R, Jackson T (2016) SMOS disaggregated soil moisture product at 1 km resolution: Processor overview and first validation results. Remote Sens Environ 180:361–376. https://doi.org/10.1016/j.rse.2016.02.045,

Morán-Tejeda, E., Herrera, S., López-Moreno, J. I., Revuelto, J., Lehmann, A., and Beniston, M.: Evolution and frequency (1970–2007) of combined temperature–precipitation modes in the Spanish mountains and sensitivity of snow cover, Reg. Environ. Change, 13, 873–885. https://doi.org/10.1007/s10113-012-0380-8, 2013

Nabat, P. S., Somot, S., Mallet, M., Sánchez-Lorenzo, A., and Wild, M.: Contribution of anthropogenic sulfate aerosols to the changing Euro-Mediterranean climate since 1980, Geophys. Res. Lett., 41, 5605–5611. https://doi.org/10.1002/2014GL060798, 2014, b

Nearing GS, Mocko DM, Peters-Lidard CD, Kumar SV, Xia Y (2016) Benchmarking NLDAS-2 soil moisture and evapotranspiration to separate uncertainty contributions. J Hydrometeorol 17(3):745–759. https://doi.org/10.1175/JHM-D-15-0063.1

Ngo-Duc, T., Polcher, J., and Laval, K.: A 53-year forcing data set for land surface models, J. Geophys. Res., 110, D06116. https://doi.org/10.1029/2004JD005434, 2005

Noilhan J, Mahfouf JF (1996) The ISBA land surface parameterisation scheme. Glob Planet Chang 13(1-4):145–159. https://doi.org/10.1016/0921-8181(95)00043-7

Noilhan J, Planton S (1989) A simple parameterization of land surface processes for meteorological models. Mon Weather Rev 117(3):536–549

Noilhan, J. and Mahfouf, J. F.: The ISBA land surface parameterisation scheme, Global Planet. Change, 13, 145–159. https://doi.org/10.1016/0921-8181(95)00043-7, 1996, b

Noilhan, J. and Planton, S.: A Simple Parameterization of Land Surface Processes for Meteorological Models, Mon. Weather Rev., 117, 536–549, 1989, b.

Olcina, J.: Tipología de sequías en España, Ería, 56, 201–227, 2001.

Owens, T., Hoddinott, J., and Kinsey, B.: Ex-Ante Actions and Ex-Post Public Responses to Drought Shocks: Evidence and Simulations from Zimbabwe, World Dev., 31, 1239–1255, https://doi.org/10.1016/S0305-750X(03)00068-8, 2003.

PaiMazumder, D., Sushama, L., Laprise, R., Khaliq, M., and Sauchyn, D.: Canadian RCM projected changes to short and long term drought characteristics over the Canadian Prairies, Int. J. Climatol., 33, 1409–1423, https://doi.org/10.1002/joc.3521, 2013.

Palmer WC (1965) Meteorological drought, vol 30. US Department of Commerce, Weather Bureau, Washington.

Palmer, W. C.: Meteorological Drought, vol. 30, US Department of Commerce, Weather Bureau Washington, DC, 1965.

Post, W. and Zobler, L.: Global soil types, 0.5-degree grid (modified zobler), Oak Ridge National Laboratory Distributed Active Archive Center, Oak Ridge, Tennessee, USA, https://doi.org/10.3334/ORNLDAAC/540, 2000.

Quintana-Seguí P, Le Moigne P, Durand Y, Martin E, Habets F, Baillon M, Canellas C, Franchisteguy L, Morel S (2008) Analysis of near-surface atmospheric variables: Validation of the SAFRAN analysis over France. J Appl Meteorol Climatol 47:92–107. https://doi.org/10.1175/2007JAMC1636.1

Quintana-Seguí P, Peral MC, Turco M, Llasat MC, Martin E (2016) Meteorological Analysis Systems in North-East Spain: Validation of SAFRAN and SPAN. J Environ Inf 27(2):116–130. https://doi.org/10.3808/jei.201600335, http://www.iseis.org/jei/abstract.asp?no=201600335

Quintana-Seguí P, Turco M, Herrera S, Miguez-Macho G (2017) Validation of a new SAFRAN-based gridded precipitation product for Spain and comparisons to Spain02 and ERA-Interim. Hydrol Earth Syst Sci 21(4):2187–2201. https://doi.org/10.5194/hess-21-2187-2017. http://www.hydrol-earth-syst-sci.net/21/2187/2017/

Quintana-Seguí, P., Barella-Ortiz, A., Regueiro-Sanfiz, S., and Míguez-Macho, G.: The Utility of Land-Surface Model Simulations to Provide Drought Information in a Water Management Context Using Global and Local Forcing Datasets, Water Resour. Manag. https://doi.org/10.1007/s11269-018-2160-9, online first, 2019, b, c, d, e

Quintana-Seguí, P.: SAFRAN analysis over Spain, ESPRI/IPSL. https://doi.org/10.14768/MISTRALS-HYMEX.1388, 2015, b

Radu, R., Déqué, M., and Somot, S.: Spectral nudging in a spectral regional climate model, Tellus A, 60, 898–910. https://doi.org/10.1111/j.1600-0870.2008.00341.x, 2008

Reichstein, M., Bahn, M., Ciais, P., Frank, D., Mahecha, M., Seneviratne, S., Zscheischler, J., Beer, C., Buchmann, N., Frank, D., Papale, D., Rammig, A., Smith, P., Thonicke, K., van der Velde, M., Vicca, S., Walz, A., and Wattenbach, M.: Climate extremes and the carbon cycle, Nature, 500, 287–295. https://doi.org/10.1038/nature12350, 2013

Ritter, B. and Geleyn, J. F.: A comprehensive radiation scheme for numerical weather prediction models with potential applications in climate simulations, Mon. Weather Rev., 120, 303–325. https://doi.org/10.1175/1520-0493(1992)1200303:ACRSFN2.0.CO;2, 1992

Rockel, B., Will, A., and Hense, A.: The Regional Climate Model COSMO-CLM (CCLM), Meteorol. Z., 17, 347–348. https://doi.org/10.1127/0941-2948/2008/0309, 2008, b

Ruiz JM (1999) Modelo distribuido para la evalución de recursos hïdricos (modelo SIMPA). Madrid, CEDEX, Ministerio de Fomento Doctorado 180.

Ruiz, J. M.: Modelo distribuido para la evaluación de recursos hídricos (modelo SIMPA), Madrid, CEDEX, Ministerio de Fomento Doctorado 180 pp., 1999, b.

Ruti, P., Somot, S., Giorgi, F., Dubois, C., Flaounas, E., Obermann, A., Dell'Aquila, A., Pisacane, G., Harzallah, A., Lombardi, E., Ahrens, B., Akhtar, N., Alias, A., Arsouze, T., Aznar, R., Bastin, S., Bartholy, J., Béranger, K., Beuvier, J., Bouffies-Cloché, S., Brauch, J., Cabos, W., Calmanti, S., Calvet, J., Carillo, A., Conte, D., Coppola, E., Djurdjevic, V., Drobinski, P., Elizalde-Arellano, A., Gaertner, M., Galán, P., Gallardo, C., Gualdi, S., Goncalves, M., Jorba, O., Jordà, G., L'Heveder, B., Lebeaupin-Brossier, C., Li, L., Liguori, G., Lionello, P., Maciàs, D., Nabat, P., Onol, B., Raikovic, B., Ramage, K., Sevault, F., Sannino, G., Struglia, M., Sanna, A., Torma, C., and Vervatis, V.: Med-CORDEX Initiative for Mediterranean Climate Studies, B. Am. Meteorol. Soc., 97, 1187–1208. https://doi.org/10.1175/BAMS-D-14-00176.1, 2016

Samaniego L, Thober S, Kumar R, Wanders N, Rakovec O, Pan M, Zink M, Sheffield J, Wood EF, Marx A (2018) Anthropogenic warming exacerbates European soil moisture droughts. Nat Clim Chang 8(5):421–426. https://doi.org/10.1038/s41558-018-0138-5

Sánchez, E., Gallardo, C., Gaertner, M., Arribas, A., and Castro, M.: Future climate extreme events in the Mediterranean simulated by a regional climate model: a first approach, Global Planet. Change, 44, 163–180, 2004, b.

Schellekens J, Dutra E, Martínez La Torre A, Balsamo G, Van Dijk A, Sperna Weiland F, Minvielle M, Calvet JC, Decharme B, Eisner S, Fink G, Flörke M, Peßenteiner S, Van Beek R, Polcher J, Beck H, Orth R, Calton B, Burke S, Dorigo W, Weedon GP (2017) A global water resources ensemble of hydrological models: The eartH2Observe Tier-1 dataset. Earth Syst Sci Data 9(2):389–413. https://doi.org/10.5194/essd-9-389-2017

Seneviratne SI, Corti T, Davin EL, Hirschi M, Jaeger EB, Lehner I, Orlowsky B, Teuling AJ (2010) Investigating soil moisture–climate interactions in a changing climate: A review. Earth-Sci Rev 99(3-4):125–161. https://doi.org/10.1016/j.earscirev.2010.02.004

Serrano, A., García, J. A., Mateos, V. L., Cancillo, M. L., and Garrido, J.: Monthly modes of variation of precipitation over the Iberian peninsula, J. Climate, 12, 2894–2919, 1999.

Sevault, F., Somot, S., Alias, A., Dubois, C., Lebeaupin-Brossier, C., Nabat, P., Adloff, F., Déqué, M., and Decharme, B.: A fully coupled Mediterranean regional climate system model: design and evaluation of the ocean component for the 1980–2012 period, Tellus A, 66, 23967, https://doi.org/10.3402/tellusa.v66.23967, 2014, b.

Sheffield J, Wood EF (2007) Characteristics of global and regional drought, 1950–2000: Analysis of soil moisture data from off-line simulation of the terrestrial hydrologic cycle. J Geophys Res 112 (D17):D17,115. https://doi.org/10.1029/2006JD008288

Sheffield J, Wood EF, Chaney N, Guan K, Sadri S, Yuan X, Olang L, Amani A, Ali A, Demuth S, Ogallo L (2014) A drought monitoring and forecasting system for Sub-Sahara african water

resources and food security. Bull Am Meteorol Soc 95(6):861–882. https://doi.org/10.1175/BAMS-D-12-00124.1

Sheffield J, Wood EF, Roderick ML (2012) Little change in global drought over the past 60 years. Nature 491(7424):435–438. https://doi.org/10.1038/nature11575

Shukla, S. and Wood, A. W.: Use of a standardized runoff index for characterizing hydrologic drought, Geophys. Res. Lett., 35, 2405. https://doi.org/10.1029/2007GL032487, 2008 a

Sousa, P. M., Trigo, R. M., Aizpurua, P., Nieto, R., Gimeno, L., and Garcia-Herrera, R.: Trends and extremes of drought indices throughout the 20th century in the Mediterranean, Nat. Hazards Earth Syst. Sci., 11, 33–51. https://doi.org/10.5194/nhess-11-33-2011, 2011, b

Sylla, M. B., Coppola, E., Mariotti, L., Giorgi, F., Ruti, P. M., Dell'Aquila, A., and Bi, X.: Multiyear simulation of the African climate using a regional climate model (RegCM3) with the high resolution ERA-interim reanalysis, Clim. Dynam., 35, 231–247. https://doi.org/10.1007/s00382-009-0613-9, 2010

Tallaksen LM, Stahl K (2014) Spatial and temporal patterns of large-scale droughts in Europe: Model dispersion and performance. Geophys Res Lett 41(2):429–434. https://doi.org/10.1002/2013GL058573

Thober S, Kumar R, Sheffield J, Mai J, Schåfer D, Samaniego L (2015) Seasonal soil moisture drought prediction over europe using the north american Multi-Model ensemble (NMME). J Hydrometeorol 16(6):2329–2344. https://doi.org/10.1175/JHM-D-15-0053.1

Tsakiris G, Pangalou D, Vangelis H (2007) Regional drought assessment based on the Reconnaissance Drought Index (RDI). Water Resour Manag 21(5):821–833

Turco, M. and Llasat, M. C.: Trends in indices of daily precipitation extremes in Catalonia (NE Spain), 1951–2003, Nat. Hazards Earth Syst. Sci., 11, 3213–3226. https://doi.org/10.5194/nhess-11-3213-2011, 2011

van der Linden, P. and Mitchell, J. F. B. (Eds.): ENSEMBLES: Climate Change and its Impacts: Summary of research and results from the ENSEMBLES project, MetOffice Hadley Centre, FitzRoy Road, Exeter EX1 3PB, UK, 160 pp., 2009.

Van Loon AF (2015) Hydrological drought explained. Wiley Interdisc Rev Water 2(4):359–392. https://doi.org/10.1002/wat2.1085

Van Loon AF, Gleeson T, Clark J, Dijk Van, AIJM Stahl K, Hannaford J, Di Baldassarre G, Teuling AJ, Tallaksen LM, Uijlenhoet R, Hannah DM, Sheffield J, Svoboda M, Verbeiren B, Wagener T, Rangecroft S, Wanders N, Van Lanen HAJ (2016) Drought in the Anthropocene. Nat Geosci 9(2):89–91. https://doi.org/10.1038/ngeo2646

Van Loon AF, Van Huijgevoort MHJ, Van Lanen HaJ (2012) Evaluation of drought propagation in an ensemble mean of large-scale hydrological models. Hydrol Earth Syst Sci 16(11):4057–4078. https://doi.org/10.5194/hess-16-4057-2012

Van Loon, A. F. and Van Lanen, H. A. J.: A process-based typology of hydrological drought, Hydrol. Earth Syst. Sci., 16, 1915–1946. https://doi.org/10.5194/hess-16-1915-2012, 2012a

Van Loon, A. F., Van Lanen, H. A. J., Hisdal, H., Tallaksen, L. M., Fendekova,M., Oosterwijk, J., Horvat, O., and Machlica, A.: Understanding hydrological winter drought in Europe, Global

Change: Facing Risks and Threats to Water Resources, 189–197, Centre for Ecology and Hydrology, Wallingford, Oxfordshire, OX10 8BB, UK, IAHS, 2010.

Van Loon, A.: Hydrological drought explained, WIREs Water, 2, 359–392. https://doi.org/10.1002/wat2.1085, 2015

Vicente-Serrano SM, Beguería S, López-Moreno JI (2010) A multiscalar drought index sensitive to global warming: The standardized precipitation evapotranspiration index. J Clim 23 (7):1696–1718. https://doi.org/10.1175/2009JCLI2909.1

Vicente-Serrano SM, Van der Schrier G, Beguería S, Azorin-Molina C, Lopez-Moreno JI (2015) Contribution of precipitation and reference evapotranspiration to drought indices under different climates. J Hydrol 526(May):42–54. https://doi.org/10.1016/j.jhydrol.2014.11.025

Vicente-Serrano, S. M. and López-Moreno, J. I.: Hydrological response to different time scales of climatological drought: an evaluation of the Standardized Precipitation Index in a mountainous Mediterranean basin, Hydrol. Earth Syst. Sci., 9, 523–533. https://doi.org/10.5194/hess-9-523-2005, 2005

Vicente-Serrano, S., Gouveia, C., Camarero, J. J., Beguería, S., Trigo, R., López-Moreno, J., Azorín-Molina, C., Pasho, E., Lorenzo-Lacruz, J., Revuelto, J., Morán-Tejeda, E., and Sánchez-Lorenzo, A.: Response of vegetation to drought timescales across global land biomes, P. Natl. Acad. Sci. USA, 110, 52–57. https://doi.org/10.1073/pnas.1207068110, 2013

Vicente-Serrano, S., López-Moreno, J. I., Beguería, S., Lorenzo-Lacruz, J., Azorín-Molina, C., and Morán-Tejeda, E.: Accurate Computation of a Streamflow Drought Index, J. Hydrol. Eng., 17, 318–332, 2012.

Vicente-Serrano, S., López-Moreno, J. I., Beguería, S., Lorenzo-Lacruz, J., Sánchez-Lorenzo, A., García-Ruiz, J. M., Azorín-Molina, C., Morán-Tejeda, E., Revuelto, J., Trigo, R., Coelho, F., and Espejo, F.: Evidence of increasing drought severity caused by temperature rise in southern Europe, Environ. Res. Lett., 9, 44001. https://doi.org/10.1088/1748-9326/9/4/044001, 2014

Vicente-Serrano, S.: Differences in spatial patterns of drought on different time scales: An analysis of the Iberian Peninsula, Water Resour. Manage., 20, 37–60. https://doi.org/10.1007/s11269-006-2974-8, 2006

Vidal JP, Martin E, Franchistéguy L, Baillon M, Soubeyroux JM (2010a) A 50-year high-resolution atmospheric reanalysis over France with the Safran system. Int J Climatol 30(11):1627–1644. https://doi.org/10.1002/joc.2003

Vidal JP, Martin E, Franchistéguy L, Habets F, Soubeyroux JM, Blanchard M, Baillon M (2010b) Multilevel and multiscale drought reanalysis over France with the Safran-Isba-Modcou hydrometeorological suite. Hydrol Earth Syst Sci 14(3):459–478. https://doi.org/10.5194/hess-14-459-2010, http://www.hydrol-earth-syst-sci.net/14/459/2010/

Vu, M., Raghavan, V., and Liong, S.: Ensemble Climate Projection for Hydro-Meteorological Drought over a river basin in Central Highland, Vietnam, Journal of Civil Engineering, 19, 427–433. https://doi.org/10.1007/s12205-015-0506-x, 2015, b

Walko RL, Band LE, Baron J, Kittel TGF, Lammers R, Lee TJ, Ojima D, Pielke Sr RA, Taylor C, Tague C, Tremback CJ, Luigi Vidale P (2000) Coupled Atmosphere–Biophysics–Hydrology

Models for Environmental Modeling. J Appl Meteorol 39:931–944. https://doi.org/10.1175/1520-0450(2000)039<0931:CABHMF>2.0.CO;2

Wanders N, Wada Y (2015) Human and climate impacts on the 21st century hydrological drought. J Hydrol 526(October):208–220. https://doi.org/10.1016/j.jhydrol.2014.10.047

Wang A, Bohn TJ, Mahanama SP, Koster RD, Lettenmaier DP (2009) Multimodel ensemble reconstruction of drought over the continental united states. J Clim 22(10):2694–2712. https://doi.org/10.1175/2008JCLI2586.1

Wang, D., Hejazi, M., Cai, X., and Valocchi, A. J.: Climate change impact on meteorological, agricultural, and hydrological drought in central Illinois, Water Resour. Res., 47, W09527. https://doi.org/10.1029/2010WR009845, 2011, b

Weedon, G., Gomes, S., Viterbo, P., Shuttleworth, W., Blyth, E., Osterle, H., Adam, J. C., Bellouin, N., Boucher, O., and Best, M.: Creation of the WATCH Forcing Data and Its Use to Assess Global and Regional Reference Crop Evaporation over Land during theTwentieth Century, J. Hydrometeorol., 12, 823–848. https://doi.org/10.1175/2011JHM1369.1, 2011

Wilhite, D. A.: Drought: a global assessment, Vols I and II, Routledge Hazards and Disasters Series, Routledge, London, UK, 2000.

Wu, C., Xian, Z., and Huang, G.: Meteorological drought in the Beijiang River basin, South China: current observations and future projections, Stoch, Environ. Res. Risk Assess., 30, 1821–1834. https://doi.org/10.1007/s00477-015-1157-7, 2016

Xu, Y., Wang, L., Ross, K. W., Liu, C., and Berry, K.: Standardized soil moisture index for drought monitoring based on soil moisture active passive observations and 36 years of north American land data assimilation system data: A case study in the southeast United States, Remote. Sens., 10, 301. https://doi.org/10.3390/rs10020301, 2018.

Yilmaz MT, Crow WT (2013) The optimality of potential rescaling approaches in land data assimilation. J Hydrometeorol 14(2):650–660. https://doi.org/10.1175/JHM-D-12-052.1